CODIGEM
CORPORACIÓN DE DESARROLLO E INVESTIGACIÓN GEOLÓGICO-MINERO-METALÚRGICA

MINISTERIO DE ENERGÍA Y MINAS

DFID
DEPARTMENT FOR INTERNATIONAL DEVELOPMENT

BGS 1835
BRITISH GEOLOGICAL SURVEY

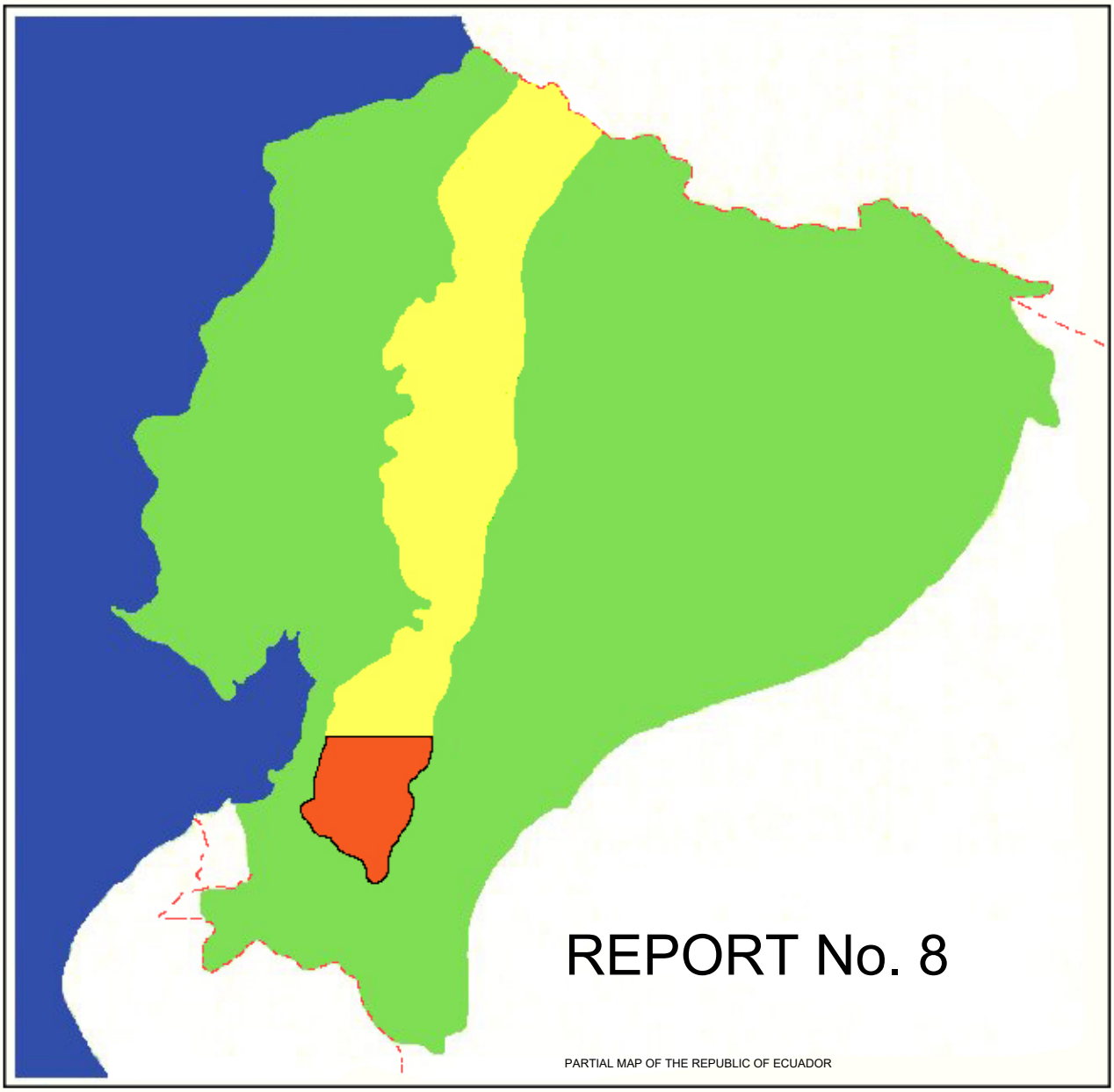

REPORT No. 8

PARTIAL MAP OF THE REPUBLIC OF ECUADOR

WORLD BANK MINING DEVELOPMENT AND ENVIRONMENTAL CONTROL PROJECT

GEOLOGICAL INFORMATION MAPPING PROGRAMME (WESTERN CORDILLERA)

PATRI MATRIQUE

CODIGEM

BGS 1835

MINING DEVELOPMENT AND ENVIRONMENTAL CONTROL PROJECT

GEOLOGICAL INFORMATION MAPPING PROGRAMME

Report Number 8

GEOCHEMICAL RECONNAISSANCE SURVEY OF THE WESTERN CORDILLERA OF ECUADOR BETWEEN 3°00' AND 4°00'S

T. M. Williams

A. Gaibor

P. N. Dunkley

CODIGEM-BRITISH GEOLOGICAL SURVEY

Quito-Ecuador

1998

Stalyn Paucar

2024 edition

GIMP GEOCHEMICAL SURVEY PROGRAMME
PARTICIPATING STAFF

Principal geochemists
Dr. T. M. Williams
Dr. P. N. Dunkley

Misión Británica manager
Dr. J. A. Aspden

CODIGEM
Ing. A. Gaibor
Mr. E. Cruz
Arq. V. Acitimbay

FIELD OPERATIONS

Group supervisor
Ing. N. Báez

Samplers
H. Durazno
F. Núñez
J. Segovia
R. Brito
H. Núñez
J. Galarza

Group supervisor
Ing. E. López

Samplers
M. Cruz
R. Rosales
J. Solis
W. Castillo
E. Hinojosa
E. Romero

Reference

Williams, T., Gaibor, A. & Dunkley, P. (1998). *Geochemical Reconnaissance of the Western Cordillera of Ecuador between 3°00' and 4°00'S* (Stalyn Paucar, Ed., 2024). Report Number 8. Geological Information Mapping Programme. BGS-CODIGEM/MEM.

CONTENTS

1. INTRODUCTION **1**

2. AREA OF COVERAGE **1**
2.1 Physiography 1
2.2 Geological setting 1
2.2.1 Metamorphic basement 1
2.2.2 Pallatanga Unit 3
2.2.3 Celica Unit 3
2.2.4 Yunguilla Unit 3
2.2.5 Quingeo Formation 3
2.2.6 Sacapalca Unit 3
2.2.7 Saraguro Group 3
2.2.8 Santa Isabel Formation 4
2.2.9 Catamayo Formation 4
2.2.10 Ayancay Group 6
2.2.11 Turi Formation 6
2.2.12 Uchucay Formation 6
2.2.13 Quimsacocha Formation 6
2.2.14 Tarqui Formation 6
2.2.15 Quaternary deposits 6
2.2.16 Intrusive rocks 7
2.2.17 Structure 7
2.3 Metalliferous mineralisation 8
2.3.1 Porphyry mineralisation 8
2.3.2 Epithermal mineralisation 8
2.3.3 Mesothermal breccias and veins 9
2.3.4 Meso-epithermal systems 9
2.3.5 Exhalative massive sulphides 9

3. SAMPLING AND ANALYTICAL PROCEDURES **10**
3.1 Numbering system 10
3.2 Field sampling procedure 10
3.3 Sample preparation 10
3.4 Analysis 11
3.4.1 Gold 11
3.4.2 Major and trace cations 11
3.4.3 Metalloids 11
3.4.4 Mercury 11

4. QUALITY CONTROL **12**
4.1 Sampling variance 12
4.2 Analytical precision 12
4.3 Control standards 14
4.3.1 GIMP control standards 14
4.3.2 BGS control standards 17
4.4 Practical detection limits 17

5. RESULTS **18**
5.1 Digital data 18
5.2 Summary statistics 18
5.3 Regional distribution of major and trace elements 18
5.3.1 Image production 18
5.3.2 Lithogeochemical terranes 18
5.3.3 Gold 19
5.3.4 Arsenic and antimony 34
5.3.5 Mercury 38
5.3.6 Copper 40

6. DISCUSSION AND CONCLUSIONS **42**
6.1 Economic potential 42
6.1.1 Interpretive guidelines 42
6.1.2 Significance of geochemical anomalies 42
6.2 Environmental baselines 43
6.2.1 Rationale 43
6.2.2 Development of sediment quality criteria 45
6.2.3 Prediction and control of mining impacts 46
6.2.4 Natural geochemical hazards 48
6.3 Concluding statement 48

7. BIBLIOGRAPHY **49**

FIGURES

1 The GIMP 3°-4°S quadrangle 2
2 Simplified geology of the GIMP 3°-4°S quadrangle 5
3 Copper and lead time-series control plots 15
4 Zinc and arsenic time-series control plots 16
Cumulative probability plot and anomaly distribution for:
5 Au 23
6 As 35
7 Sb 37
8 Hg 39
9 Characteristic pH and dissolved contaminant characteristics of mine-waters 47
10 Spidergrams for selected mineral deposits 47

TABLES

1	Sampling variance data	12
2	Precision thresholds for selected elements	13
3	BGS certification of control standards	14
4	Bondar Clegg and independently determined analytical detection limits	17
5	Geochemical data for the Cordillera Occidental 3°-4°S area: summary statistics	20
6	Geochemical data for the Cordillera Occidental 3°-4°S area. Pearson correlation matrix	21
	Summary statistics of:	
7	Metamorphic basement	24
8	Pallatanga Unit	25
9	Celica Unit	26
10	Sacapalca Unit	27
11	Saraguro Group	28
12	Ayancay Group	29
13	Quimsacocha Formation	30
14	Turi Formation	31
15	Tarqui Formation	32
16	Major granodiorite and diorite intrusions	33
17	Summary of principal drainage anomalies	43
18	Sediment Quality Criteria for the Protection of Aquatic Life	45

1. INTRODUCTION

The Geological Information Mapping Programme (GIMP) of the Misión Geológica Británica incorporates sub-components 3.3 and 3.4 of the wider Mining Development and Environmental Control Project (PRODEMINCA), initiated in Ecuador in 1995 under funding from the World Bank (loan no. 3655 EC) and the governments of Ecuador, the United Kingdom and Sweden. The central function of the GIMP is to produce geological maps and thematic geoscience data for the Cordillera Occidental of Ecuador, for use by the Ministry of Energy and Mines in the promotion of sustainable mineral sector investment.

The GIMP geological and thematic survey encompasses a 36000 km^2 area of the Cordillera Occidental between latitudes 1°N and 4°S. This report summarises the methodology and results of drainage reconnaissance of the 3°-4°S quadrangle (see cover illustration), sampling of which was undertaken between September and November 1996.

All data contained in this report have been incorporated into a digital release package in accordance with the requirement of many prospective users to undertake independent data interpretation in a wide range of software applications. A series of 1:200000 scale single element maps has also been prepared, and may conveniently be viewed in conjunction with this text.

2. AREA OF COVERAGE

2.1 Physiography

The 3°-4°S quadrangle of the Cordillera Occidental extends between longitudes 79°-80°E, covering approximately 6200 km^2. Major settlements include Loja, Zaruma, Pasaje, Saraguro, Piñas and San Fernando (Fig. 1). The Panamerican Highway, connecting Cuenca and Loja, provides the region's principal N-S access route, with the Cuenca-Santa Isabel-Pasaje road forming the main E-W artery. Access to the sector north of the Río Jubones is poor.

2.2 Geological setting

A 1:200000 scale geological map of the 3°-4°S of the Cordillera Occidental has been produced under the GIMP and published by BGS-CODIGEM (1997). A detailed account of the lithostratigraphy, structure and mineralisation of the area is provided by Pratt et al. (1997). A simplified geological map based on the above work is provided in Fig. 2.

2.2.1 Metamorphic basement

Metamorphic rocks, the continuation of the El Oro metamorphic complex (Aspden et al., 1995; Feininger, 1973), probably underlie much of the area. Largely concealed by younger volcanic lithologies northeast of the Jubones Fault, they occur in erosional windows such as San Pablo de Cebadas, Manú and in the Río San Luis. Metasediments predominate, including very low grade (sub-greenschist) slates and cleaved conglomerates. Higher grade facies (gneisses and foliated garnet-bearing granitic gneisses) occur at Manú and San Pablo de Cebadas. In the far south of the mapped area, andalusite and biotite grade strata pass southward into unmetamorphosed turbidites of the El Tigre Unit (Aspden et al., 1995).

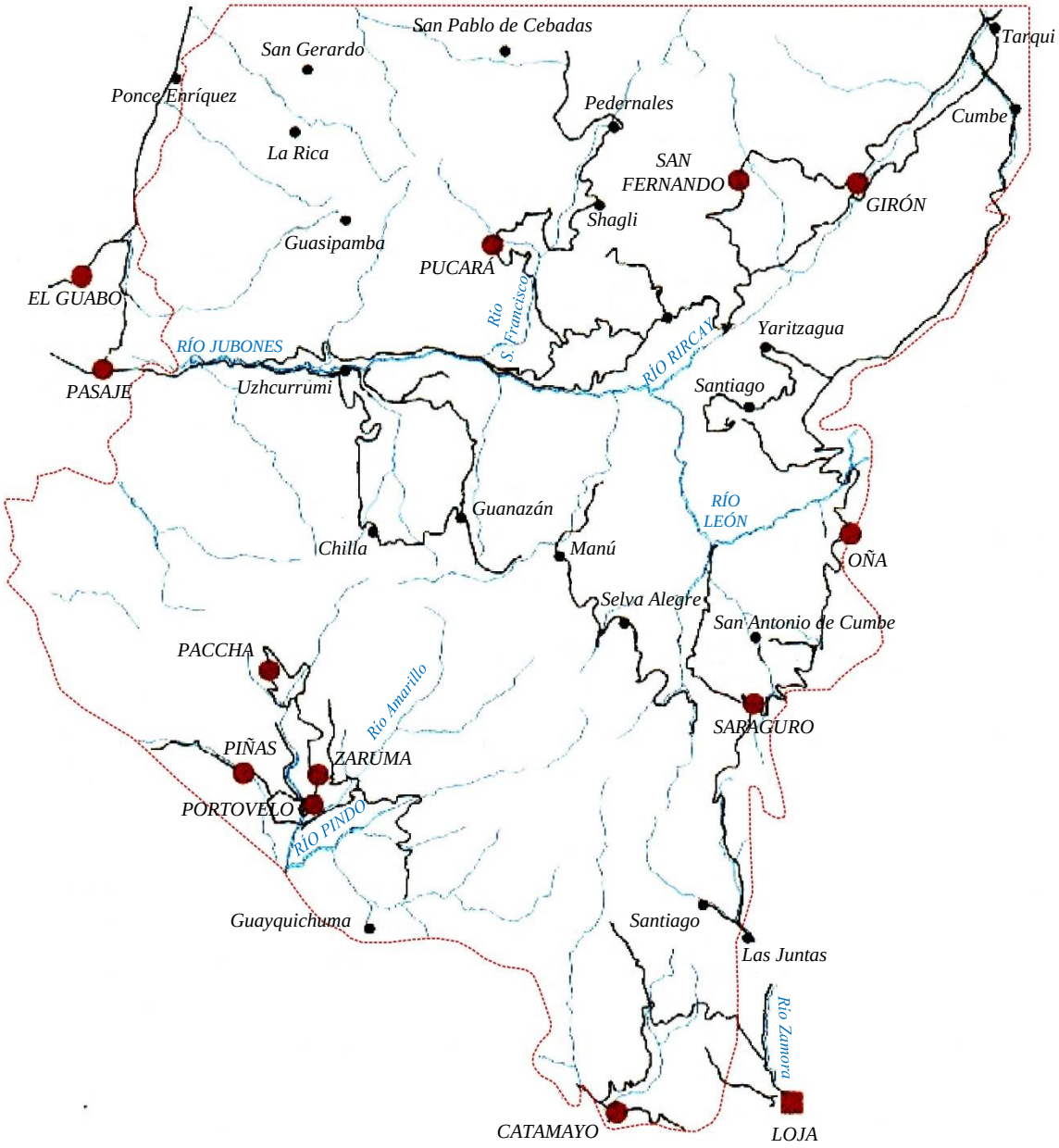

Figure 1. The GIMP 3°-4°S quadrangle

2.2.2 Pallatanga Unit

The Pallatanga Unit (McCourt et al., 1997) comprises blue-green basalts and hyaloclastites, best exposed around Bella Rica and Tres Ranchos in the north-west of the mapped area. The rocks show pervasive hydrothermal alteration with epidote, chlorite, calcite and disseminated pyrite. The unit is tentatively assigned a mid-Cretaceous age.

2.2.3 Celica Unit

The Celica Unit (Pratt et al., 1997) crops out in the south-east of the area, fault-bounded between the metamorphic basement and Sacapalca Unit. The lithologies comprise deeply weathered green andesitic tuffs and lavas, rich in plagioclase, amphibole and augite crystals. Stratigraphic relationships suggest an Albian age (Jaillard et al., 1996).

2.2.4 Yunguilla Unit

The Yunguilla Unit (cf. Hughes and Bermúdez, 1997) comprises a marine turbidite fan sequence, exposed in inliers at Cumbe, south of Cuenca, and between Selva Alegre and Manú. A biostratigraphically-based Maastrichtian age has been assigned to the unit (Woods, 1997).

2.2.5 Quingeo Formation

The Quingeo Formation is exposed at Cumbe. It overlies the Yunguilla Unit, with which it is in apparent transitional contact. It comprises a sequence of purple sandstones, siltstones and mudstones. A Maastrichtian age has been suggested for the base of the Formation (Pratt et al., 1997; Woods, 1997). In the type-section, however, Steinmann (1997) assigned a Middle to Late Eocene age.

2.2.6 Sacapalca Unit

The Sacapalca Unit (Pratt et al., 1997) outcrops widely in the east and south-east. It comprises andesite lavas, tuffaceous breccias, conglomerates, lacustrine mudstones and sparse dacitic tuffs. According to Pratt et al. (1997), it is intruded by the San Lucas pluton (59-51 Ma; Aspden et al., 1992) and the El Tingo intrusion (47 ± 2 Ma; 50 ± 3 Ma; Kennerley, 1980), consistent with a Palaeocene or Early Eocene age (Jaillard et al., 1996). A fission track age of 66.9 ± 5.8 Ma obtained from near Catacocha implies a latest Maastrichtian or early Palaeocene age.

2.2.7 Saraguro Group

The Saraguro Group (Baldock, 1982) occupies some 60% of the mapped area and is best exposed between Tenguelillo and the páramo around Quinuas and Narihuiña (west of San Fernando). The group comprises dacitic to rhyolitic welded ash-flow tuffs with intercalations of andesites, reworked volcanic material and sedimentary rocks. In the Quinuas area, the lower 1 km of the sequence has sparse turbidite mudstone and sandstone intercalations. The Saraguro Group of the 3°-4°S area spans the Eocene to mid-Miocene, incorporating the following Units/Formations:

2.2.7.1 The Las Trancas Formation (Pratt et al., 1997) can be traced westwards from the Las Trancas type area to the coastal plain south of Ponce Enríquez. The main lithologies are andesitic/dacitic lithic lapilli-tuffs, tuffaceous breccias, conglomerates, red mudstones and sandstones. Metamorphic fragments, including gneiss and schist, are common.

2.2.7.2 The Portovelo Unit (Pratt et al., 1997) outcrops to the north of the Piñas-Portovelo Fault. It comprises basaltic-andesite and andesite lavas and andesite tuffs. Geochemical data indicate a calc-alkaline signature.

2.2.7.3 The Jubones Formation (Pratt et al., 1997) occurs near the top of the Saraguro Group. The outcrop indicates an original extent of at least 2700 km^2 with a maximum thickness of 500 m. The southernmost exposures occur in a narrow graben at Guanazán, and the northernmost, about 60 km to the north, at Pimo (Dunkley and Gaibor, 1997b). The Formation is rich in plagioclase, biotite and quartz crystals. Large scale (>1 m diameter) cooling joints and a weak welding foliation are widespread. A co-ignimbrite breccia lag and base surge with silicified trees occur at the type locality. Near Santa Isabel, the tuff has been dated by K/Ar (biotite) as earliest Miocene (22.76 ± 0.97 Ma).

2.2.7.4 The La Fortuna Formation (Pratt et al., 1997) covers at least 450 km^2. Geochemically and petrographically it is similar to the Jubones Tuff but with a greater amount of fine matrix (vitroclasts). The Formation is dated by fission track to 23.2 Ma.

2.2.7.5 The La Paz Formation (Pratt et al., 1997) covers an area of about 600 km^2 and is restricted to the east of the Girón Fault System. The main outcrop is in the páramo between La Paz (the type locality), Oña and Saraguro. The tuff is crystal-rich, with abundant large quartz and plagioclase crystals. A fission track age of 22.5 ± 0.9 Ma (Early Miocene) has been obtained.

2.2.8 Santa Isabel Formation

The Santa Isabel Formation (Pratt et al., 1997) crops out in the area of Santa Isabel and Girón, fringing the Ayancay Group. The strata are mainly calcite-veined andesitic tuff-breccias and lavas. Fission track dating has established an Early Miocene age for the Formation (Hungerbühler, in prep.).

2.2.9 Catamayo Formation

The Catamayo Formation (Jaillard et al., 1996) crops out around Catamayo. It comprises red and yellow sandstones, siltstones and mudstones, unconformably overlying the Sacapalca andesites. A tentative Middle Miocene age has been assigned.

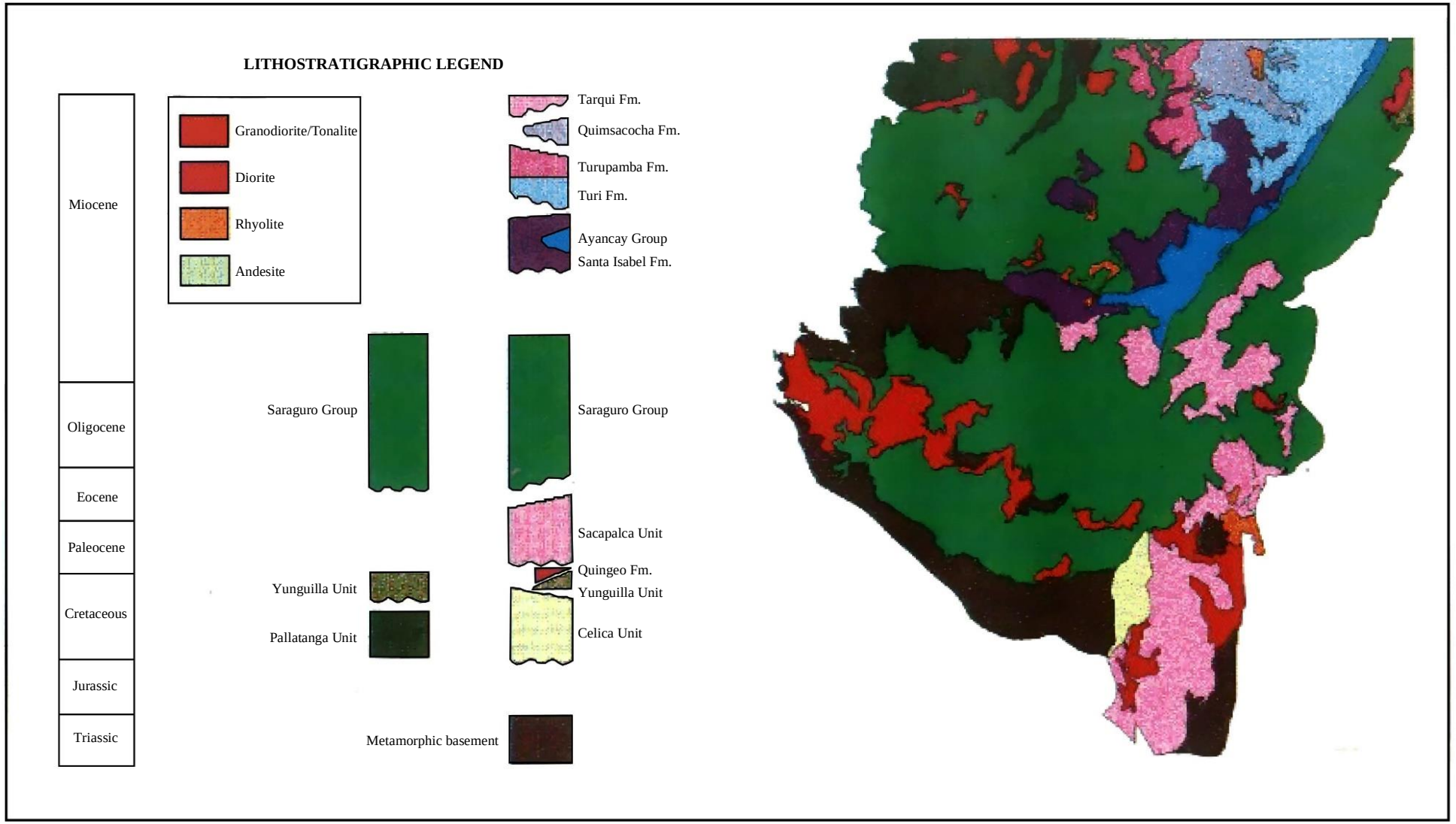

Figure 2. Simplified geology of the GIMP 3°-4°S quadrangle

2.2.10 Ayancay Group

The Ayancay Group (UNDP, 1969) is largely confined to a zone between the Girón Fault System and the Gañarín Belt. The sequence is sandwiched between the upper tongues of andesite of the Santa Isabel Formation, thinning northwards. The most northerly exposures occur at Tuncay to the east of the Gañarín Belt. Lithologies comprise reddish conglomerates, sandstones, siltstones and mudstones with rare air-fall tuffs and coals. Deposition spanned much of the Miocene.

2.2.11 Turi Formation

The Turi Formation (Erazo, 1957) outcrops to the north of the Girón Fault System and to the east of the Gañarín Belt. The geometry of the outcrop is radial, dipping southward and eastward away from the Quimsacocha Caldera. The main lithologies are tuffaceous breccias, conglomerates and sandstones, rich in andesite debris with sporadic andesitic tuff-breccias. Fission track dates indicate a Late Miocene age (8-9 Ma).

2.2.12 Uchucay Formation

The Uchucay Formation (DGGM, 1973) is confined to the Santa Isabel area. It comprises yellow conglomerates and boulder beds with a diverse assemblage of locally-derived clasts. Fission track dates infer a Late Miocene age (9.4 ± 0.8 Ma).

2.2.13 Quimsacocha Formation

The Quimsacocha Formation (Pratt et al., 1997) caps the Turi Formation around the Quimsacocha Caldera. Like the Turi, the outcrop is radial with gentle dips away from the Caldera. The strata are very fresh plagioclase-phyric lavas. A post-Late Miocene age is inferred by stratigraphic relations with the Turi Formation.

2.2.14 Tarqui Formation

The Tarqui Formation (UNDP, 1969) crops out mainly on the eastern slopes of the Quimsacocha centre and in the páramo between Oña and Saraguro. It blankets all older Formations unconformably and reaches a maximum thickness of about 400 m west of Saraguro. The Quimsacocha exposures comprise deeply weathered acid tuffs. In contrast, north of Saraguro, the rocks are mainly thinly bedded tuffs (some of them air-fall) tuffaceous conglomerates and tuffaceous sandstones. Plant remains are common and there are rare coals. The Tarqui Formation is intruded by sub-volcanic dacite intrusions at Saraguro, dated by fission track to 9.6 ± 0.5 Ma.

2.2.15 Quaternary Deposits

Alluvial valley-fills are common in the principal drainage channels, and more extensive cover sequences drape rocks of Cretaceous to Tertiary age over lower parts of the mapped area adjacent to the coastal plain. Colluvial deposits are mapped to the north of Manú.

2.2.16 Intrusive rocks

Dolerites and gabbros occur within, and are interpreted to be part of the Pallatanga Unit. Metamorphic rocks, and deeper levels of the Saraguro Group and Sacapalca Unit are extensively intruded by quartz diorites and granodiorites (tonalites) in the southern and western sectors of the mapped area. The granitoids are typically coarse to medium grained, and show evidence of quenching (interstitial chloritised glass, fine granophyric and holocrystalline intergrowths), consistent with high-level emplacement. The Paccha intrusion, covering an area of at least 150 km^2, has been dated by K/Ar methods to 16.89 ± 0.16 Ma. K/Ar dates of 19.92 ± 0.18 Ma and 17.64 ± 0.61 Ma have been determined for a quartz diorite northeast of Uzhcurrumi [6635-96347] and the Shagli granodiorite intrusion respectively.

Sub-volcanic stocks of aphyric rhyolite and porphyritic andesite are common within the Saraguro Group and younger Formations, notably in the area of the inferred Jubones Caldera and along the Gañarín Belt. Some may be transitional into domes, for example at Abañín [6675-96316]. Along the Santa Isabel to Pucará road [6726-96407], a brecciated rhyolite up to 300 m thick and with a strike length of 5 km may represent a collapsed dome. Generally, subvolcanic complexes become younger towards the northeast. Rhyolites around Pachagmama are probably latest Oligocene/earliest Miocene, while those within the Quimsacocha Caldera (intruding the Turi Formation) must be younger than 10 Ma.

2.2.17 Structure

The NNE-striking Chaucha-Río Jérez Lineament is marked by a belt of faults, folds, steeply dipping strata and metamorphic inliers, traceable from Chaucha (north of the mapped area) to the San Pablo de Cebadas inlier. The western margin of this inlier is defined as a reverse fault which brings the Pallatanga Unit over the Saraguro Group. Farther south, it is not clear if this structure runs into the La Tigrera Fault, or into a belt of anomalously steep, east-dipping Saraguro Group tuffs extending from Narihuiña through the polymetallic prospects of Tres Chorreras and Gigantones to Uzhcurrumi [6550-96350].

The Girón Fault System comprises tight folds, reverse faults and thrusts which strike north-NNE. A thrust at La Cría brings the Sacapalca Unit and Saraguro Group over the Ayancay Group. The La Cría Anticline is interpreted as a fold above a blind, NW-verging thrust. The Yaritzagua Syncline is strongly NW-verging, with a vertical, to overturned, east limb.

The Girón Fault System links with the east-striking Jubones Fault System. In the east the latter thrusts the Sacapalca Unit over the Ayancay Group. A thrust plane, overlain by Sacapalca andesites and underlain by the overturned Jubones Formation and Ayancay Group, is exposed in the Río Manú.

The NNE-striking Gañarín Belt can be traced from Zaruma in the south of the mapped area, to Quimsacocha close to the 3°S line. It comprises a series of syn-depositional faults which exert an important regional control on regional volcanism and metallogenesis. This structure may constrain the west side of the Cuenca Basin and explain the presence of hot springs and travertine deposits at Baños, southwest of Cuenca.

Several ESE-striking faults occur in the northwest of the area within the Pallatanga Unit. None appear to have a major throw and they die out rapidly in younger, Saraguro Group strata. A serpentinite outcrop of uncertain origin occurs along the NW-SE striking Río Chico Fault.

2.3 Metalliferous mineralisation

An outline of the economic geology of the 3°-4°S area of the Cordillera Occidental is provided by Pratt et al. (1997). The principal documented mineral occurrences are summarised below.

2.3.1 Mineralised porphyritic and non-porphyritic rhyolite-andesite stocks

Gaby [ref. 6428-96620] constitutes the principal known porphyry occurrence in the mapped area. Intense argillic alteration, with Mo-Cu-Au mineralisation in stockworks and disseminations, is recorded in association with a minor microdiorite stock (Gemuts et al., 1992; Paladines and Rosero, 1996). A possible porphyry occurrence at Fierro Urcu [ref. 6830-95916] is associated with a complex of sill-like granodiorites and strongly jointed microdiorites, apparently cut by a younger rhyolite, within country rocks of the Saraguro Group. Additional localities noted by Pratt et al. (1997) as hosting evidence of porphyry-style mineralisation include Salvias [ref. 6593-96011], Shagli [ref. 6806-96497] and Cerro Nudillo [ref. 6680-95888].

2.3.2 Epithermal mineralisation associated with calderas, rhyolite stocks and regional fractures

The north-east-striking Gañarín Belt hosts several epithermal prospects of predominantly low-sulphidation character. The structure extends 60 km from the Guanazán Au prospect (west of Manú) to Baños (south-west of Cuenca). The belt has exerted an important control on the emplacement of sub-volcanic complexes and domes, and the position of eruptive centres such as Quimsacocha and Jubones. Intrusive bodies were emplaced over a time-span of >15 million years, ranging from ca. 26 for the Pachagmama rhyolite to <10 Ma for the Quimsacocha rhyolite. Rhyolitic intrusions are typically characterised by argillic alteration, silicification and disseminated pyrite mineralisation. A crystal-poor texture suggests that the fluids may, in several cases, have represented the final phases of magma chamber purging, with consequent enrichment of volatiles and metals.

At Quimsacocha [ref. 6978-96645], the most northerly Gañarín Belt prospect within the mapped area, rhyolites are characterised by local argillic alteration and disseminated pyrite mineralisation. A high sulphidation signature is observed relative to other Gañarín Belt prospects (alunite-enargite). Cinnabar occurs within the assemblage. The Cañaribamba prospect [ref. 6860-96437], north of Santa Isabel, is associated with a rhyolite dome, with limited alteration and possible sinter-type mineralisation. At Gañarín [ref. 6795-96355], a silicified cap some 40m thick overlies andesitic tuffs and breccias of the Santa Isabel Andesites, cross-cut by NNE striking quartz veins carrying up to 12-15 g/t Au. At Pachagmama [ref. 6750-96315], a rhyolite intrusion forms the heart of the Jubones Caldera. It is identical in aspect to the Quimsacocha intrusion, showing localised argillic (kaolin) alteration and disseminated pyrite mineralisation. Propylitic alteration (epidote, calcite, chlorite) is evident on the east flank of a plagioclase amphibole-phyric andesite stock at Trigopamba [ref. 6758-96290], with disseminated pyrite recorded in adjacent Saraguro Group tuffs. In the Zaruma/Portovelo district, the Gañarín Belt passes to the west side of the Salvias metamorphic inlier [6600-95960]. A few km to the SW, mineralised sub-volcanic rhyolite stocks and adjacent andesites are variably silicified and argillically altered, with attendant pyrite mineralisation.

2.3.3 Mesothermal breccias and veins

Mesothermal mineralisation within the mapped area is typically associated with breccias or tourmaline dykes at (granodiorite) intrusive margins. The Tres Chorreras prospect [ref. 6637-96505], currently a site of artisanal mining, comprises irregular stocks of feldspar-, amphibole- and quartz-phyric microdiorite intruded into lithic tuffs and welded rhyolitic tuffs of the Saraguro Group. Mineralised breccias occur within the intrusive facies close to the tuff contact, beyond which a large halo of disseminated tourmaline extends for several hundred metres. The typical assemblage includes massive molybdenite, hematite, chalcopyrite, pyrite and tourmaline. The distribution of mineralisation at Tres Chorreras is dictated by competence, with intrusion-tuff contacts constituting sites of increase tectonic fracturing. There is no evidence that the host breccias are of hydrothermal origin. The La Playa Mine [ref. 6520-96430], 12 km SW of Tres Chorreras, comprises several sub-vertical breccia pipes within a granodiorite cupola. The cupola is extremely close to the contact with the La Fortuna Formation, a major angular unconformity. Mineralisation may, therefore, reflect some form of fluid barrier. Each pipe is roughly 100 m in diameter and comprises tourmaline-quartz breccia with variable contents of metal sulphides and oxides (notably chalcopyrite, specular hematite, sphalerite and bornite, with secondary malachite and azurite). Fine-grained Au occurs free and within sulphides. Grades of Au are typically 2-4 g/t with ca. 40 g/t Ag. An additional mined breccia pipe at La Tigrera [ref. 6512-96446] is located in the same granodiorite intrusion as those at La Playa. The pipe is vertical, and lies at the contact of the intrusive cupola and tuffs of the La Fortuna Formation. Additional (probable) mesothermal occurrences associated with quartz-tourmaline pods, pipes and dykes include Uzhcurrumi [ref. 6636-96476], Paccha [ref. 6488-96045] and Selva Alegre [ref. 6736-95988].

2.3.4 Base metal-poor auriferous mesothermal veins with epithermal overprints

Two historically important mining areas within the 3°-4°S sector of the Cordillera Occidental show evidence of co-existing mesothermal and epithermal mineralisation. At Zaruma-Portovelo, swarms of N-S trending auriferous veins occur within rhyolite stocks and surrounding andesites. The Misión Belga (1989) recognised two phases of mineralisation, the first characterised by Au plus base metal sulphides (pyrite, chalcopyrite, sphalerite, galena, bornite, covellite) with deposition temperatures of 320-380°C. A later, lower temperature phase, is base-metal poor with high non-refractory Au contents. The absence of alunite and the presence of adularia in the wallrocks suggest a low sulphidation character. Van Thournout et al. (1991) have suggested that propylitic alteration in the Zaruma-Portovelo region is confined to a circular zone, ca. 9 km in diameter, possibly related to a former eruptive centre. The two distinct phases of mineralisation are thus interpreted as pre-caldera and post-caldera events. At Bella Rica-Tres Ranchos mesothermal veins occur within the Pallatanga Unit in the northwest of the mapped area. Disseminated pyrite and pyrite stockworks are widespread in a zone of extensive propylitic alteration. The most important mineralisation occurs in the Bella Rica concession [e.g. ref. 6448-96588], a system of NNW-trending veins some 3 km long, with a known width of 400 m. The metalliferous assemblage comprises pyrite, pyrrhotite, arsenopyrite, sphalerite, galena and hematite. Visible Au is rare.

2.3.5 Exhalative massive sulphides

Sulphide-rich mineralisation west of San Fernando [ref. 6886-96558] was drilled during a UNDP reconnaissance northeast investigation (UNDP, 1969) and interpreted as of low temperature exhalative character.

3. SAMPLING AND ANALYTICAL PROCEDURES

3.1 Numbering system

A random numbering system based on that of Plant (1973) and Garrett (1983) was deployed throughout the Cordillera Occidental geochemical survey to preclude analytically-induced campaign boundaries (within or between sheet areas) and/or the generation of spurious multiple-sample anomalies. Prior to sampling the project area, several thousand sample bags were sequentially numbered, randomized and issued. On return to the CODIGEM laboratory, all filled samples bags were re-ordered and forwarded for analysis in sequential batches of ca. 120 samples. Through this procedure short-term analytical fluctuations (affecting one or more sample batches) are manifested as analytical noise across the entire project area, rather than as discrete local or sub-regional trends.

3.2 Field sampling procedure

Drainage sediment samples were collected by two sampling teams, each comprising eight trained prospectors. Samples were collected during five commissions, each lasting three weeks, during dry season conditions (May-December). A total of 2390 samples was collected from a ca. 6200 km^2 area, representing an average resolution of 1 sample per 2.59 km^2. In all instances emphasis was placed on the recovery of samples from first or second order regimes, thus constraining relatively small provenance areas.

The sampling methodology deployed throughout the Cordillera Occidental survey was derived from that of Plant and Moore (1979), and is broadly compliant with the global IGCP 259/360 protocol for International Geochemical Mapping (Darnley et al., 1995). Sampling stations were located upstream of potential sources of perturbation (habitation, industrial activity, agricultural discharges or bridging structures). At each site several kilograms of active channel detritus were collected following the removal of the hydrous-oxide enriched interfacial horizon. The alluvium was then wet-screened through an 80 BSI mesh (177μm) sieve using a minimum volume of water so as to avoid the loss of fine silt and clay fractions. Following a settling period of ca. 20 minutes, the clear water overlying the sediment was decanted and approximately 100 g of the remaining sediment was transferred to a pre-numbered kraft bag for transport and storage.

The selection of an 80 BSI sediment fraction for use throughout the survey was based on an orientation study by Dunkley et al. (1997) in the Río Junín basin. The fraction effectively reflects both mechanical and hydromorphic dispersion signatures (e.g. Williams et al., 1992) and avoids the logistic problem of collecting a sufficient mass of finer (100 BSI or smaller) material from the high-energy drainage systems which characterise much of the higher ground of the Cordillera Occidental.

3.3 Sample preparation

On return from the field all samples were air-dried at <40°C thus precluding any loss of Hg or other volatile elements. Samples were then disaggregated with a pre-washed pestle and mortar to yield a fine homogeneous powder. This was sub-sampled using a cone-and-quarter technique to produce a ca. 50 g aliquot for multi-element analysis.

3.4 Analysis

Chemical analyses of sediments were performed in the Vancouver laboratories of Bondar Clegg Ltd. using four independent methods.

3.4.1 Gold

Samples of 30 g were analysed for Au by fire-assay with subsequent determination of the fused product by atomic absorption spectrophotometry (AAS).

3.4.2 Major and trace cations

A suite of 34 major and trace cations (Ag, Cu, Pb, Zn, Mo, Ni, Co, Cd, Bi, As, Sb, Fe, Mn, Te, Ba, Cr, V, Sn, W, La, Al, Mg, Ca, Na, K, Sr, Y, Ga, Li, Nb, Sc, Ta, Ti, Zr) was simultaneously determined by inductively-coupled plasma emission spectroscopy (ICP-ES) following the digestion of 1.0 g aliquots in 100 ml of aqua-regia (ARISTAR). The use of aqua-regia rather than an HF-based total dissolution method reflects the superior peak/background responses to mineralisation obtained during orientation studies undertaken by the Misión Geológica Británica at Junín (Dunkley et al., 1997).

3.4.3 Metalloids

On account of the low resolution (5 mg/kg in solid) of metalloid analyses by ICP-ES, additional data for As and Sb were obtained by hydride-generation AAS. A flow-injection (FIA) introduction system of Nakashima (1979) facilitated the reduction of As to arsine and injection into the aspiration chamber simultaneously by merging a flow of 0.2% $NaBH_2$ with the sample carrier.

3.4.4 Mercury

Total Mercury was determined by cold-vapour AAS (CVAAS) following aqua-regia digestion of 1.0 g sediment aliquots under hot-reflux.

4. QUALITY CONTROL

4.1 Sampling variance

For 31 elements the statistical variance attributable to at-site sediment heterogeneity and/or sampling bias was calculated for the entire Cordillera Occidental survey area using a modified analysis of variance (ANOVA) technique (Plant et al., 1975). Duplicate sediment samples acquired through repeat sampling of selected drainage sites (at a maximum frequency of 2 per 100) were analysed, and the results were used to determine sampling variance using the sums of squares technique (Bolviken and Sinding-Larsen 1973). In instances where both duplicates from a single site yielded sub-detection limit values, the record was excluded from the calculation. Summary statistics are provided in Table 1. Statistical F-tests are not quoted, as the data do not fully satisfy the assumptions of conventional ANOVA analysis. It requires emphasis that the sampling variance data are themselves derived from the *analytical* determination of field duplicates. The values therefore assume interpretative significance only when in excess of the corresponding analytical precision threshold.

Table 1. Sampling variance data, based on ANOVA analysis of duplicate samples from selected field stations within the Cordillera Occidental survey area.

Element	%variance	Element	%variance	Element	%variance	Element	%variance
Ag	7.1	**Sn**	15.2	**As**	3.1	**Ga**	11.6
Cu	3.1	**W**	21.7	**Sb**	6.9	**Y**	21.2
Pb	7.1	**La**	4.3	**Fe**	6.6	**Nb**	15.4
Zn	4.7	**Al**	3.6	**Mn**	7.1	**Sc**	16.0
Mo	25.0	**Mg**	7.1	**Bi**	17.5	**Ti**	4.4
Ni	12.4	**Ca**	12.5	**Ba**	3.2	**Zr**	12.1
Co	3.5	**Na**	12.2	**Cr**	9.3	**Hg**	21.7
Cd	4.2	**K**	9.4	**V**	4.9		

4.2 Analytical precision

Precision (p) is an index of the reproducibility of analytical determinations conventionally defined as:

$$p = \left(\frac{2s}{x}\right) * 100\%$$

The term is distinguishable from accuracy, which reflects the relationship between an individual determination or group of determinations and the true matrix composition. In exploration, indices of analytical precision are critical as they provide an insight into inter-comparability of data for individual samples or sample batches.

Analytical precision data for the 3°-4°S and 2°-3°S quadrangles were derived from two statistical exercises based on the duplicate analysis of aliquots of homogenized sediment (Plant et al., 1975; Thompson and Howarth, 1978). The first entailed a calculation of the variation of the standard deviation (s_c) across an empirically-defined concentration range (c) in accordance with the linear function:

$$s_c = s_0 + kc$$

where s_0 is the standard deviation at zero concentration and k is the gradient of the straight line. Values for S_0 and k were obtained by:

(i) Determination of mean $\frac{x^1+y^1}{2}$ and absolute difference (x^1-y^1) values for all duplicate pairs.

(ii) Ranking of duplicate pairs by ascending mean.

(iii) Calculation for the 'mean of means' and 'median of differences' for discrete groups of 11 duplicate pairs (8 groups = 88, with 3 discarded).

(iv) Regression of median against mean values determined in (iii) to yield s_0 (intercept) and k (gradient).

The second method utilised a series of precision control charts on which 90th and 99th percentile concordance lines were plotted for one or more pre-determined precision levels. Practically acceptable precision thresholds defined by the latter method, and systematically applied to quality control of the analytical output for the 3°-4°S quadrangle, have been reported by Dunkley and Gaibor (1997a) and are summarised in Table 2.

Table 2. Precision thresholds for selected elements applied for quality-control of analytical data for the 3°-4°S Cordillera Occidental quadrangle (from Dunkley and Gaibor, 1997a)

Element	%variance	Element	%variance
Ag	25	**As**	5
Cu	20	**Sb**	10
Pb	40	**Mn**	15
Zn	20	**Fe**	15
Mo	25	**V**	40
Ni	10	**Sr**	25
Co	15	**Cd**	15
Ba	20	**Li**	15
Cr	10	**Bi**	20

4.3 Control standards

4.3.1 GIMP control standards

Three control standards derived from fluvial sediments within the project area (Junín River, J-1; Angamarca River, COR-1; hybrid sample, M-1) were characterised at the UK laboratories of the British Geological Survey by a combination of ICP-ES, ICP mass spectrometry (ICP-MS) and X-ray fluorescence (XRF) methods at the outset of the Cordillera Occidental survey (Table 3). With the exception of J-1 which contains anomalous concentrations of Cu (>95th %ile of the 3°-4°S dataset), plus moderately high As and Sb, these standards hold background concentrations of most elements of economic interest.

During the analysis of samples from the 3°-4°S area, additional control standards derived from mineralised localities at Ponce Enríquez (PE), Cerro Negro (CN), and a mixture of these plus lower background samples (M-2) were introduced. Repeat analyses undertaken by Bondar Clegg show the Ponce Enríquez standard to be highly anomalous with respect to a range of metals/metalloids, including As (mean 1476 mg/kg), Cu (mean 1062 mg/kg) and Au (mean 2.62 mg/kg). The Cerro Negro standard is strongly enriched in Cu (mean 398 mg/kg), Pb (125 mg/kg), Mo (44 mg/kg) and Sb (289 mg/kg) relative to the empirical dataset for the 3°-4°S area.

Table 3. BGS certification of control standards J-1, COR-1, and M-1, based on the mean of analysis by multiple techniques

Element	BGS value (ppm)			Element	BGS value (ppm)		
	J-1	COR-1	M-1		J-1	COR-1	M-1
Ag	<0.2	<0.2	<0.2	**As**	12.5	5.0	7.0
Cu	175	23	79.5	**Sb**	3.3	0.6	1.4
Pb	3.5	5.0	7.0	**Mn**	468	375	413
Zn	61	43	50.5	**Fe (%)**	4.9	8.1	7.0
Mo	1.6	0.5	1.0	**V**	150	293	226
Ni	10.5	18.5	14.0	**Sr**	28.5	61.0	48.0
Co	10.7	14.8	12.9	**Cd**	ND	1.0	0.5
Ba	74	64.5	73	**Li**	5.9	6.0	5.5
Cr	44.5	82.0	65.0				

Two sub-samples of three or more control standards were submitted blind to Bondar Clegg with each batch of 120 field samples. The resultant data provided a basis for evaluating (i) instrumental accuracy and (ii) temporal drift. The latter was evaluated independently of precision (4.2 above) as it commonly involves a systematic adjustment, thus amenable to correction. Analytical data for all Cordillera Occidental control standards are reported by Williams et al. (1997).

The impact of systematic instrumental drift on the Cordillera Occidental 3°-4°S dataset was evaluated using conventional time-series plots, as exemplified in Figs. 3-4. In rare instances in which control-standard values concurrently deviated by more than 2 standard deviations from the mean, an appropriate correction was applied. Examples exist in the time-series data shown for Zn, in which the values for standards submitted with analytical batches 22-24 are systematically depressed.

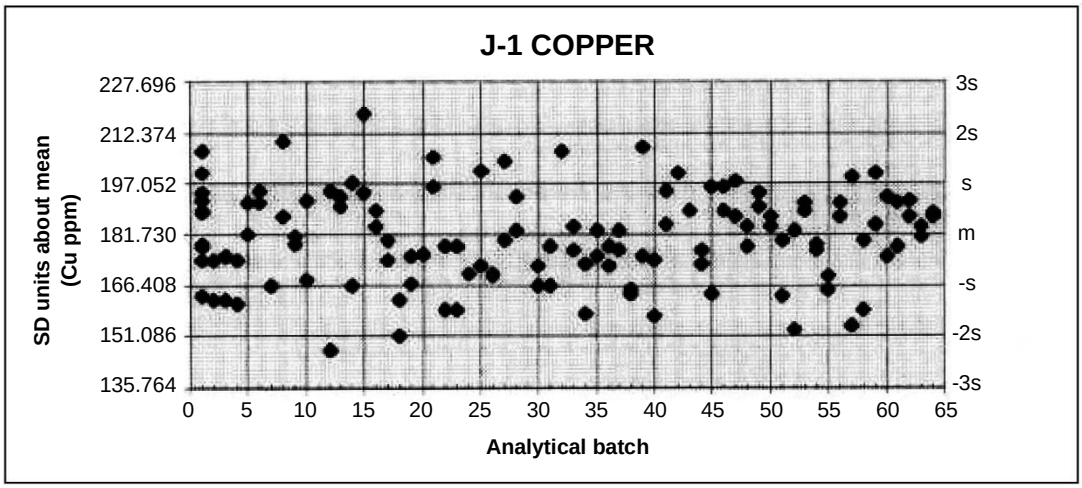

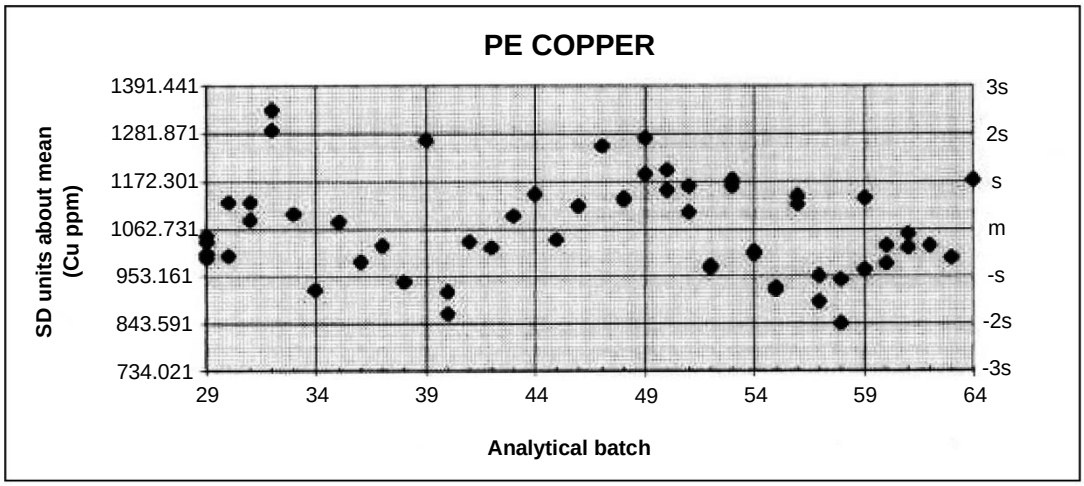

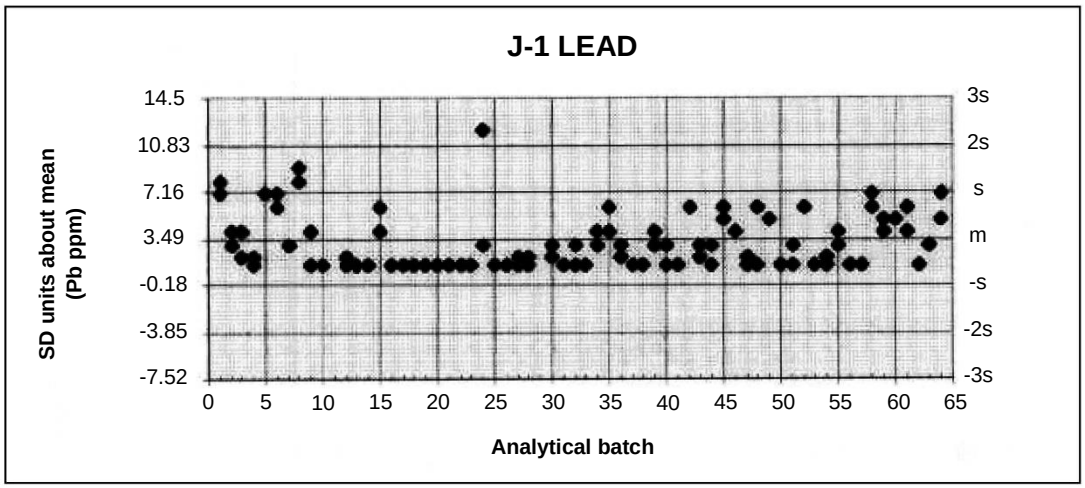

Figure 3. Copper and lead time-series control plots showing the results of replicate analyses of simultaneous duplicate pairs of Ecuadorian reference sediments. Correction of the empirical dataset is applied under the GIMP only in instances where BOTH samples within a duplicate pair deviate from the mean by >2SD for any individual sample batch.

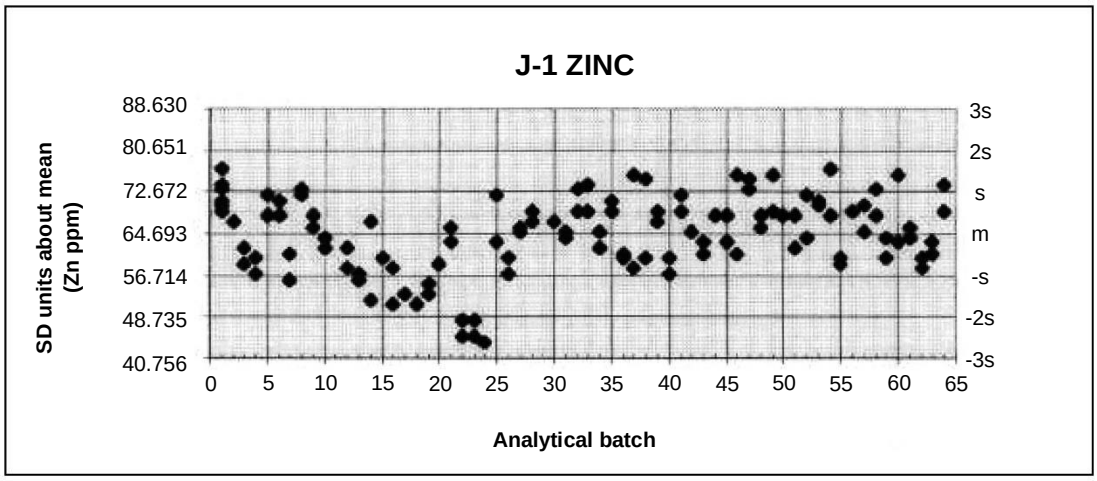

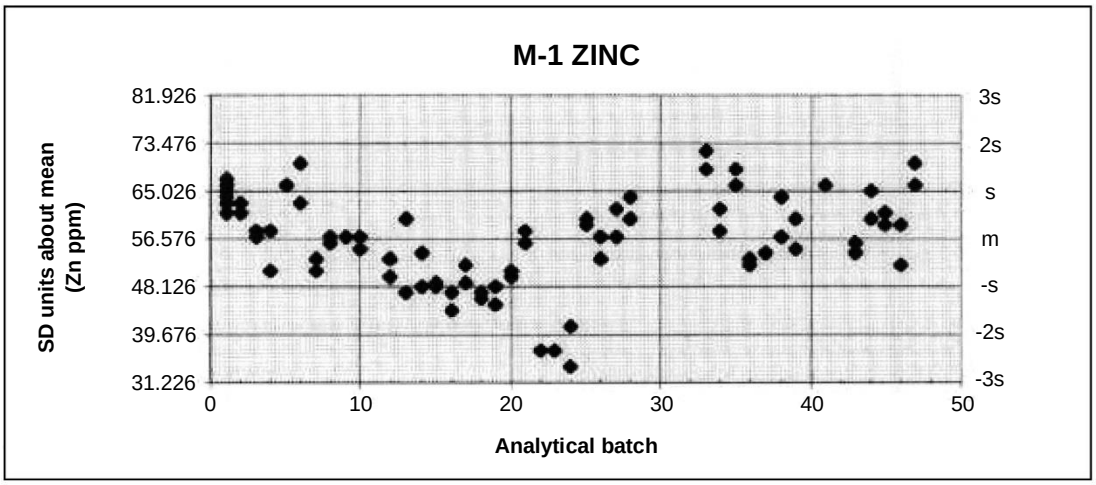

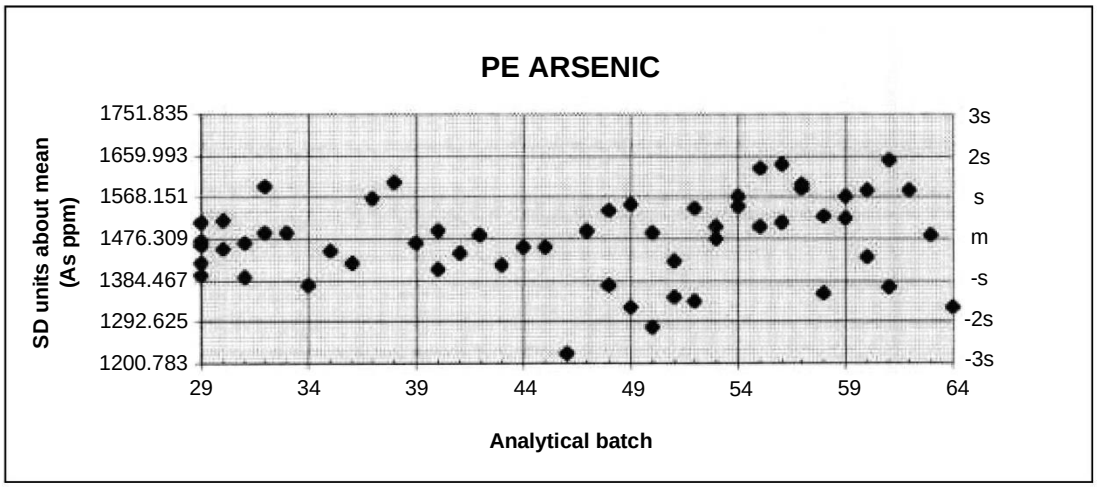

Figure 4. Zinc and arsenic time-series control plots showing the results of replicate analyses of simultaneous duplicate pairs of Ecuadorian reference sediments. Correction of the empirical dataset is applied under the GIMP only in instances where BOTH samples within a duplicate pair deviate from the mean by >2SD for any individual sample batch. An example is provided by the Zn data for batches 22-24.

4.3.2 BGS control standards

In addition to the project control standards described, BGS reference standards S13, S15, S24 and S3B were submitted for analysis by Bondar Clegg. These standards were derived from 100 BSI stream sediments from geologically varied British terrains. All have been analysed in several European laboratories by a combination of XRF, AAS, ICP-ES, ICP-MS and DRES methods. Inter-laboratory comparisons for these samples are provided by Williams et al. (1997). Relatively high values for elements such as Pb reflect the use by BGS of a total analytical technique (XRF) rather than the partial (aqua-regia digestion) method of Bondar Clegg.

4.4 Practical detection limits

With the exception of Au, analytical detection limits (LODs) provided by Bondar Clegg were not adopted for use in the validation of geochemical data as they do not account for the matrix influences typically encountered during the analysis of geological materials. Practical LODs for each element were instead determined using two methods. The first involved the replicate analysis of reference samples over a range of concentrations, and the regression of the standard deviation against the mean concentration for each value to yield a value of the standard deviation at zero concentration (s_0). A LOD of $3s_0$ was then calculated in accordance with UIPAC (1978). The second method involved the derivation of s_0 using the method of Thompson and Howarth (1978), as outlined in section 4.2. Results of LOD determinations acquired using both techniques are given in Table 4, with the adopted value highlighted in each case.

Table 4. Bondar Clegg and independently determined analytical detection limits (adopted values highlighted). All values are in mg/kg unless otherwise indicated.

Element	Bondar Clegg	Extrapolation Method	Thompson and Howarth
Ag	0.2	**1.0**	0.9
Au	0.05	-	-
As	1	6.1	**4.5**
Ba	1	**5.4**	2.4
Bi	5	**6.0**	-
Cd	0.2	**0.7**	1.4
Cr	1	**3.7**	4.7
Co	1	**2.6**	1.9
Cu	1	**4.5**	11.0
Fe	0.01%	**0.3%**	0.6%
Hg	0.01	**0.04**	0.04
Li	1	**1.2**	1.0
Mn	1	**34.0**	-
Mo	1	**1.35**	5.0
Ni	1	**3.3**	2.4
Pb	2	**4.0**	12.0
Sb	0.2	1.9	**0.74**
Zn	1	**5.0**	15.0

5. RESULTS

5.1 Digital data

The digital data release package for the Cordillera Occidental 3°-4°S quadrangle holds 2930 records each comprising a sample number, locational data (UTM SAD59 coordinates) and error-controlled analytical output for 36 elements in tab-delineated text format.

5.2 Summary statistics

Descriptive statistics for the multi-element dataset for the 3°-4°S quadrangle are provided in Table 5. Cumulative frequency data indicate that populations for most elements are skewed and poorly amenable to non-parametric statistical analysis. Pearson (R) correlation analyses of log-normalised data (Table 6) highlight spatial covariation between several major and trace analytes. Gold is strongly covariant with Ag (R 0.613), Cu (R 0.657), Bi (R 0.599), As (R 0.645) and Sb (R 0.515). The utility of these elements as Au pathfinders is thus considered much greater than reported for the 2°-3°S sector of the Cordillera Occidental (Williams et al., 1997), within which low correlations between Au and metalloids (R <0.2) prevail. The presence of several polymetallic mesothermal assemblages is indicated by significant correlations between Pb, Zn and Cu (R 0.443-0.926). Covariation between a suite of elements with mafic affinities (notably Mg, Cr, Ni) is recorded.

5.3 Regional distribution of major and trace elements

5.3.1 Image production

The 1:200000 geochemical maps produced to accompany this report show the distribution of major and trace elements within the 3°-4°S area using six colour classifiers superimposed onto a drainage base. Gridded surfaces (inset) were generated using an inverse-distance weighting (IDW) algorithm within the MapInfo sub-component Vertical Mapper, onto which geological lines (corresponding to the simplified lithostratigraphy shown in Fig. 2) were subsequently placed in DXF format.

5.3.2 Lithogeochemical terranes

The maps produced for all analysed major and trace elements display excellent co-registration of lithology and sediment geochemistry, consistent with limited hydromorphic dispersion. The major lithotectonic terranes are well differentiated, including the basement (characteristically potassic), oceanic basalts of the Pallatanga Unit (K background < 0.05%, Ba <40 mg/kg, Cr, Ni, Mg and V levels within the upper 5 %ile of the 3°-4°S dataset) and the Sacapalca Unit (high backgrounds of Ca 0.75-2.75%; Mg ca. 0.9%). Within the Saraguro Group, the Portovelo Unit yields high Mg/Ca ratios, with high backgrounds of Cr (ca. 35 mg/kg) and Zn (ca. 100 mg/kg) relative to other member formations. Rhyolitic and dacitic lithologies (e.g. Jubones and La Paz Formations) appear as negative features with respect to these elements. Within the central sector of the mapped area, the intensely calcite-veined andesites of the Santa Isabel Formation are conspicuous, yielding median values of Ca, Mg and V within the upper 10%ile of the entire dataset, and sporadically high backgrounds for Ni, Zn and Cr.

Due to the lithogeochemical heterogeneity of the 3°-4°S area, the application of a single suite of statistically-defined background, threshold and anomaly values is inappropriate as a basis for exploration. Lithological normalization, deployed previously for the 2°-3°S sector of the Cordillera Occidental (Williams et al., 1997a), facilitates the illucidation of subtle geochemical features which may otherwise be difficult to resolve. A statistically-based procedure for normalised anomaly derivation has been applied to the 3°-4°S dataset using the exploration data processing software Interdex (Visidata Ltd.). A geo-registered display of sample points overlain by a DXF file of polygonised lithologies was used to isolate stations within selected polygons. Cumulative probability plots were then generated for individual elements in each unit, and inflections used to identify threshold and anomaly values within the population.

Summary statistics for all major lithostratigraphic units are provided in Tables 7-16. It requires emphasis that several of the polygons utilised to define these units incorporate minor intrusion, inliers and outliers of often contrasting lithology. The statistical data presented in Tables 7-16 must thus be interpreted as representative of litho-tectonic terranes, rather than of the named lithostratigraphic units *sensu stricto*.

5.3.3 Gold

Cumulative probability data for Au within the 3°-4°S area (Fig. 5) depict a background of <45 μg/kg (73 %ile) with a secondary threshold of ca. 560 μg/kg (95 %ile) and several strongly anomalous outliers in excess of 1495 μg/kg (97 %ile).

Gold occurrences within the Río Santa Rosa (in the south-west of the mapped area) show possible evidence of a basement source, although small Saraguro Group outliers could also provide a plausible host. The catchment headwaters cut intruded volcanics of the Saraguro Group, but drainage Au values in these upper reaches are routinely low (<20 μg/kg). Four stations with eastern and western limits of 629054-9603631 (sample 2691) and 625715-9603977 (sample 5862) respectively yield values of 275-1835 μg/kg Au, with enrichment of Cu to 1835 mg/kg, Ag to 10.4 mg/kg, Bi to 32 mg/kg, As to 2880 mg/kg and Sb to 67 mg/kg.

The Pallatanga Unit outcrop bounded to the east by Q. Mangán hosts Au values to 443 μg/kg (sample 4287, ref. 669071-9666579), with Cu to 129 mg/kg, Bi to 13 mg/kg and As to 109 mg/kg. These occurrences show a clear association with minor intrusive stocks which, in turn, display a strong structural control. The larger Bella Rica-San Gerardo tract yields numerous anomalous Au values, the precise origins of which are obscured by perturbation from artisanal mining. The mean Au value for this polygon (including minor intrusives) is 819 μg/kg, with a median in excess of 100 μg/kg. In the Estero Guanache system, four values in excess of 3000 μg/kg are recorded (sites 788, 30, 657, 744) downstream of the Gaby porphyry. Station 744 [ref. 642324-9661716], within 1 km of Gaby, yields 9351 μg/kg Au, 17.3 mg/kg Ag, 4264 mg/kg Cu, 1832 mg/kg Pb, 105 mg/kg Bi, 10000 mg/kg As, 113 mg/kg Sb and 1.3 mg/kg Hg. Such values are additionally influenced by the exploitation of NNW-trending mesothermal vein swarms at Bella Rica to the south-east. In the Río Blanco-Río Negro system, 4 values of 1389-2776 μg/kg Au (sites 628, 878, 278, 977) occur downstream of artisanal operations, with attendant enrichment of Cu to 2478 mg/kg, Bi to 60 mg/kg and As to 540 mg/kg. Mines in the San Gerardo district produce values up to 8675 μg/kg Au, with up to 6138 mg/kg As, 306 mg/kg Sb, 33 mg/kg Cd and 3.2 mg/kg Hg close to the margin of a diorite stock in the NW-trending Río Chico. A lower-temperature assemblage is indicated relative to that prevailing in the Bella Rica block, with a markedly lower Cu presence, high Cd and Sb.

Table 5. Geochemical data for the Cordillera Occidental 3°-4°S area. Summary statistics

	Count	Mean	Std. Dev	Min	Max	Median
Au	2390	139.205	723.032	3.33	10000*	3.33
Ag	2390	1.092	3.711	0.66	87	0.66
Cu	2390	108.866	835.057	3	20000*	20
Pb	2390	38.605	196.657	2.66	6732	17
Zn	2390	116.992	292.839	3.33	8516	80.78
Mo	2390	8.539	136.806	0.9	4458	0.9
Ni	2390	15.589	32.387	2.2	850.5	9
Co	2390	14.409	16.277	1.73	462.037	12
Cd	2390	1	4.934	0.46	137.1	0.46
Bi	2390	5.042	7.383	4	203.5	4
Fe	2390	4.022	1.704	0.33	10*	3.81
Mn	2390	831.126	444.884	41	11890	775.5
Te	2390	7.009	4.452	6.66	169.5	6.66
Ba	2390	157.007	96.68	3	1333	136
Cr	2390	31.648	39.671	2.46	854.5	22
V	2390	93.147	64.711	2	747.5	77
Sn	2390	13.48	1.708	13.33	56	13.33
W	2390	14.538	27.457	13.33	844.5	13.33
La	2390	11.857	7.383	0.66	103	11
Al	2390	2.939	1.11	0.19	9.48	2.83
Mg	2390	0.671	0.401	0.007	4.02	0.65
Ca	2390	0.57	0.672	0.007	10*	0.41
Na	2390	0.029	0.034	0.007	0.4	0.02
K	2390	0.121	0.093	0.007	1.14	0.09
Sr	2390	44.011	40.96	-1	308	32
Y	2390	7.404	3.35	0.66	35	7
Ga	2390	5.01	3.625	1.33	36	4.5
Li	2390	13.26	8.286	0.8	61	12
Nb	2390	2.3	2.758	0.66	51	1
Sc	2390	5.796	3.46	3.33	36	5
Ta	2390	6.869	3.623	6.66	146.33	6.66
Ti	2390	0.085	0.067	0.007	0.58	0.07
Zr	2390	3.717	4.202	0.66	37	2
As	2390	76.103	544.178	2.66	10000*	12.1
Sb	2390	4.956	45.134	1.26	2000*	1.26
Hg	2390	0.251	2.056	0.026	50*	0.056

Table 6. Cordillera Occidental sector 1°-2°S. Pearson correlation matrix

	Au	Ag	Cu	Pb	Zn	Mo	Ni	Cd	Bi	Fe	Mn	Te	Ba	Cr	V	Sn	W	Al	Mg	Ca	K	Sr	Y	Li	Ti	Zr	As	Sb	Hg
Au	***1.000***	**0.613**	**0.657**	0.354	0.323	**0.457**	0.125	**0.453**	**0.599**	0.267	0.019	0.355	-0.148	0.083	0.007	0.074	0.154	-0.119	0.064	0.019	-0.044	-0.115	-0.051	-0.062	-0.062	-0.070	**0.645**	**0.516**	0.171
Ag	**0.613**	***1.000***	**0.771**	**0.774**	**0.742**	**0.494**	0.008	**0.628**	**0.755**	0.253	0.046	0.314	-0.127	-0.027	-0.052	0.147	0.211	-0.143	-0.045	-0.040	-0.030	-0.090	-0.069	-0.056	-0.094	-0.050	**0.401**	**0.502**	0.078
Cu	**0.657**	**0.771**	***1.000***	**0.502**	**0.443**	**0.775**	0.026	**0.470**	**0.614**	0.274	0.026	0.335	-0.129	-0.006	-0.022	0.127	0.175	-0.131	-0.029	-0.034	-0.028	-0.086	-0.052	-0.072	-0.069	-0.048	**0.405**	**0.413**	0.080
Pb	0.354	**0.774**	**0.502**	***1.000***	**0.926**	0.092	0.011	**0.756**	**0.665**	0.204	0.073	**0.435**	-0.106	-0.018	-0.027	0.234	0.014	-0.083	-0.027	-0.045	-0.039	-0.079	-0.050	-0.017	-0.071	-0.040	**0.418**	0.158	0.054
Zn	0.323	**0.742**	**0.443**	**0.926**	***1.000***	0.020	0.011	**0.741**	**0.641**	0.251	0.154	0.346	-0.122	-0.001	0.021	0.200	0.003	-0.050	0.016	-0.037	-0.043	-0.074	-0.025	0.025	-0.024	-0.027	0.344	0.118	0.054
Mo	**0.457**	**0.494**	**0.775**	0.092	0.020	***1.000***	-0.010	0.027	0.206	0.150	0.015	0.010	-0.059	-0.033	-0.042	-0.001	0.107	-0.095	-0.064	-0.018	0.003	-0.042	-0.031	-0.058	-0.052	-0.037	0.104	**0.650**	0.066
Ni	0.125	0.008	0.026	0.011	0.011	-0.010	***1.000***	0.045	0.043	0.202	0.056	0.051	-0.179	**0.836**	0.121	0.033	-0.010	0.066	**0.581**	0.014	0.053	-0.147	0.064	0.102	0.118	-0.065	0.136	0.029	0.092
Cd	**0.453**	**0.628**	**0.470**	**0.756**	**0.741**	0.027	0.045	***1.000***	**0.714**	0.202	0.056	**0.618**	-0.110	0.014	-0.003	0.283	0.004	-0.076	0.033	0.001	-0.045	-0.072	-0.049	-0.024	-0.058	-0.038	**0.644**	0.182	0.059
Bi	**0.599**	**0.755**	**0.614**	**0.665**	**0.641**	0.206	0.043	**0.714**	***1.000***	0.292	0.020	**0.703**	-0.141	0.003	0.018	0.345	0.082	-0.117	0.008	-0.047	-0.062	-0.104	-0.087	-0.058	-0.072	-0.055	**0.653**	0.315	0.076
Fe	0.267	0.253	0.274	0.204	0.251	0.150	0.202	0.202	0.292	***1.000***	0.317	0.173	-0.315	0.385	**0.752**	0.092	0.106	0.279	0.389	0.019	-0.121	-0.117	0.089	0.115	0.368	0.069	0.206	0.157	0.028
Mn	0.019	0.046	0.026	0.073	0.154	0.015	0.056	0.056	0.020	0.317	***1.000***	-0.015	0.149	0.087	0.220	0.009	-0.019	0.182	0.193	0.141	-0.103	0.106	0.262	0.107	0.122	0.043	$-9.131*10^{-5}$	0.013	0.003
Te	0.355	0.314	0.335	**0.435**	0.346	0.010	0.051	**0.618**	**0.703**	0.173	-0.015	***1.000***	-0.091	0.002	0.042	**0.475**	0.003	-0.081	0.023	-0.007	-0.056	-0.043	-0.050	-0.046	-0.007	-0.027	**0.637**	0.114	0.049
Ba	-0.148	-0.127	-0.129	-0.106	-0.122	-0.059	-0.179	-0.110	-0.141	-0.315	0.149	-0.091	***1.000***	-0.212	-0.130	-0.056	-0.025	0.056	-0.266	0.043	0.200	**0.471**	0.095	-0.203	-0.009	0.246	-0.123	-0.070	-0.019
Cr	0.083	-0.027	-0.006	-0.018	-0.001	-0.033	**0.836**	0.014	0.003	0.385	0.087	0.002	-0.212	***1.000***	0.355	0.041	-0.017	0.160	**0.627**	0.004	0.075	-0.177	0.097	0.135	0.262	-0.054	0.066	0.001	0.053
V	0.007	-0.052	-0.022	-0.027	0.021	-0.042	0.121	-0.003	0.018	**0.752**	0.220	0.042	-0.130	0.355	***1.000***	0.023	-0.005	0.189	0.307	0.136	-0.132	0.145	-0.032	-0.092	**0.665**	0.318	0.016	-0.027	0.006
Sn	0.074	0.147	0.127	0.234	0.200	-0.001	0.033	0.283	0.345	0.092	0.009	**0.475**	-0.056	0.041	0.023	***1.000***	0.016	0.020	0.021	-0.027	-0.013	-0.055	-0.058	-0.003	0.001	-0.036	0.175	0.037	0.021
W	0.154	0.211	0.175	0.014	0.003	0.107	-0.010	0.004	0.082	0.106	-0.019	0.003	-0.025	-0.017	-0.005	0.016	***1.000***	-0.048	-0.007	-0.025	0.027	0.034	0.042	-0.030	-0.027	-0.029	0.038	0.091	0.003
Al	-0.119	-0.143	-0.131	-0.083	-0.050	-0.095	0.066	-0.076	-0.117	0.279	0.182	-0.081	0.056	0.160	0.189	0.020	-0.048	***1.000***	0.273	-0.034	-0.019	0.015	0.198	0.295	0.229	0.209	-0.099	-0.076	-0.007
Mg	0.064	-0.045	-0.029	-0.027	0.016	-0.064	**0.581**	0.033	0.008	0.389	0.193	0.023	-0.266	**0.627**	0.307	0.021	-0.007	0.273	***1.000***	0.280	0.200	0.013	0.133	0.383	0.249	-0.111	0.082	-0.018	0.026
Ca	0.019	-0.040	-0.034	-0.045	-0.037	-0.018	0.014	0.001	-0.047	0.019	0.141	-0.007	0.043	0.004	0.136	-0.027	-0.025	-0.034	0.280	***1.000***	-0.004	**0.536**	0.122	-0.049	0.119	0.223	0.034	0.006	-0.004
K	-0.044	-0.030	-0.028	-0.039	-0.043	0.003	0.053	-0.045	-0.062	-0.121	-0.103	-0.056	0.200	0.075	-0.132	-0.013	0.027	-0.019	0.200	-0.004	***1.000***	0.025	0.212	0.365	0.023	-0.222	-0.047	-0.008	-0.061
Sr	-0.115	-0.090	-0.086	-0.079	-0.074	-0.042	-0.147	-0.072	-0.104	-0.117	0.106	-0.043	**0.471**	-0.177	0.145	-0.055	0.034	0.015	0.013	**0.536**	0.025	***1.000***	0.019	-0.217	0.229	**0.472**	-0.082	-0.057	-0.003
Y	-0.051	-0.069	-0.052	-0.050	-0.025	-0.031	0.064	-0.049	-0.087	0.089	0.262	-0.050	0.095	0.097	-0.032	-0.058	0.042	0.198	0.133	0.122	0.212	0.019	***1.000***	0.339	-0.003	0.017	-0.038	-0.041	-0.050
Li	-0.062	-0.056	-0.072	-0.017	0.025	-0.058	0.102	-0.024	-0.058	0.115	0.107	-0.046	-0.203	0.135	-0.092	-0.003	-0.030	0.295	0.383	-0.049	0.365	-0.217	0.339	***1.000***	-0.092	-0.333	-0.056	-0.046	-0.032
Ti	-0.062	-0.094	-0.069	-0.071	-0.024	-0.052	0.118	-0.058	-0.072	0.368	0.122	-0.007	-0.009	0.262	**0.665**	0.001	-0.027	0.229	0.249	0.119	0.023	0.229	-0.003	-0.092	***1.000***	**0.562**	-0.067	-0.055	0.039
Zr	-0.070	-0.050	-0.048	-0.040	-0.027	-0.037	-0.065	-0.038	-0.055	0.069	0.043	-0.027	0.246	-0.054	0.318	-0.036	-0.029	0.209	-0.111	0.223	-0.222	**0.472**	0.017	-0.333	**0.562**	***1.000***	-0.043	-0.040	0.022
As	**0.645**	**0.401**	**0.405**	**0.418**	0.344	0.104	0.136	**0.644**	**0.653**	0.206	$-9.131*10^{-5}$	**0.637**	-0.123	0.066	0.016	0.175	0.038	-0.099	0.082	0.034	-0.047	-0.082	-0.038	-0.056	-0.067	-0.043	***1.000***	0.294	0.068
Sb	**0.516**	**0.502**	**0.413**	0.158	0.118	**0.650**	0.029	0.182	0.315	0.157	0.013	0.114	-0.070	0.001	-0.027	0.037	0.091	-0.076	-0.018	0.006	-0.008	-0.057	-0.041	-0.046	-0.055	-0.040	0.294	***1.000***	0.064
Hg	0.171	0.078	0.080	0.054	0.054	0.066	0.092	0.059	0.076	0.028	0.003	0.049	-0.019	0.053	0.006	0.021	0.003	-0.007	0.026	-0.004	-0.061	-0.003	-0.050	-0.032	0.039	0.022	0.068	0.064	***1.000***

2390 observations were used in this computation

Over the Saraguro Group, high Au values occur principally in the Zaruma-Portovelo area, to the west of the postulated Jubones Caldera (Pratt et al., 1997), and in the Gañarín Belt between San Fernando and San Sebastián. At Zaruma, several values in excess of 1000 μg/kg Au are recorded in the south-flowing Río Salado-Río Calera system, trending sub-parallel to the intruded contact of andesites of the Portovelo Unit and undifferentiated Saraguro Group rocks. At site 3651 [ref. 650514-9598121] a value of 3835 μg/kg Au shows attendant enrichment of Pb (334 mg/kg), Cu (336 mg/kg), Cd (6.7 mg/kg) and As (397 mg/kg), some 2 km east of Muluncay and 200 m north of a small rhyolite emplacement. At station 6041 [ref. 694590-9598008] a value of 9446 μg/kg Au occurs with 48 mg/kg Ag, 5472 mg/kg Cu, 664 mg/kg Pb, 2156 mg/kg Zn, 21 mg/kg Cd, 121 mg/kg Bi and 520 mg/kg As, probably related to mesothermal polymetallic assemblages again associated with the emplacement of a minor rhyolite stock. Several km to the west of the Río Calera, an Au anomaly of 6798 μg/kg with >50 mg/kg Hg is recorded in the S flowing Q. Honda (sample 6227, ref. 655585-9594969).

Undifferentiated Saraguro Group rocks to the west of the Jubones Caldera (Pratt et al., 1997) host numerous Au anomalies, mostly attributable to documented mineralisation. At Tres Chorreras the northern limit of mineralisation is marked by an Au value of 9561 μg/kg (site 813, ref. 663781-9649831) in the SSW-flowing Río Gigantes, with an alteration halo characterised by disseminated tourmaline. The anomalous assemblage includes 931 mg/kg Cu, 87 mg/kg Mo, 222 mg/kg As and 3.2 mg/kg Sb. Approximately 1500 m further south (close to the upper Tres Chorreras 'glory hole'), values of 7520-9292 μg/kg Au are accompanied by markedly higher Au concentrations (>50 mg/kg), up to 2% Cu, 4458 mg/kg Mo, 2388 mg/kg As, 60 mg/kg Bi, 2000 mg/kg Sb and 4.4 mg/kg Hg (e.g. site 1714, ref. 663959-9649821; site 988, ref. 663356-9648122). The highest Cu and Mo concentrations coincide with a microdiorite-brecciated tuff contact, characterised by intense argillic alteration and abundant disseminated pyrite. Analogous mineralisation to the SW of Tres Chorreras is indicated by concentrations of Au to 3837 μg/kg with high concentrations of Cu and Mo at stations in the Río Gigantes and tributary drainage (site 190, ref. 660295-9644770; site 326, ref. 659775-9645029), close to the Gigantones prospect.

Polymetallic mineralisation at La Playa (12 km SW of Tres Chorreras) is associated with a series of NW-trending breccia pipes, and highlighted by a drainage anomaly in the Río Las Juntas (site 303, ref. 651549-9640288) close to the contact of the Saraguro Group with the granodiorite intrusion which hosts the mineralised breccias. A concentration of 2140 μg/kg Au occurs within the Cu-Mo-Bi-As-Sb rich assemblage. Strong W enrichment (778 mg/kg) is consistent with the presence of scheelite (Pratt et al., 1997). Approximately 6 km south of La Playa, an analogous drainage signature (3415 μg/kg Au, 24 mg/kg Ag, 3353 mg/kg Cu, 171 mg/kg Mo, 20 mg/kg Bi, 844 mg/kg W, 569 mg/kg As, 38 mg/kg Sb) illucidates further mineralisation associated with an independent granodiorite outcrop close to Mollepungu (site 304, ref. 651435-9637102).

An Au concentration in excess of the 10000 μg/kg analytical reporting limit was recorded at station 180 [ref. 657523-9638731] in a zone of intruded porphyritic andesites in the Río Vivar system, 5 km south of the La Chorrera workings. The site is characterised by strong enrichment of Cu (17470 mg/kg) and Mo (2169 mg/kg), plus As, Sb and Hg.

Prospects in the NNE-trending Gañarín Belt are variably highlighted by drainage Au anomalies. Notable examples occur in the Río Naranjo to the east of Cañaribamba (site 1914, ref. 688215-9644903) where values of 3046 μg/kg Au and 9.6 mg/kg Ag occur in a base-metal poor assemblage. Close to the Gañarín prospect, a value of 1045 μg/kg Au was recorded in a similarly base-metal poor assemblage in the Río Minas system (site 518, ref. 680680-9635202).

Post-Saraguro volcanic sequences host few drainage Au anomalies and typically have a low-background. In the vicinity of Quimsacocha, auriferous mineralisation is highlighted by a modest drainage response in Q. Quinuahuaycu (Au 266 μg/kg) at the western margin of the caldera.

Relatively few pronounced Au anomalies occur within the major intrusive tracts of the 3°-4°S area. The most conspicuous is near Paccha (site 3714, ref. 648821-9605120), where a concentration of 5749 μg/kg Au is coincident with intense enrichment of a broad suite of metals (54 mg/kg Ag, 10000 mg/kg Cu, 4210 mg/kg Pb, 5727 mg/kg Zn, 137 mg/kg Cd, 203 mg/kg Bi, 53 mg/kg Sn, 10000 mg/kg As, 168 mg/kg Sb, 5.5 mg/kg Hg). Mineralisation in association with one or more mineralised tourmaline breccia pipes within the granodiorite host complex constitutes the perceived source.

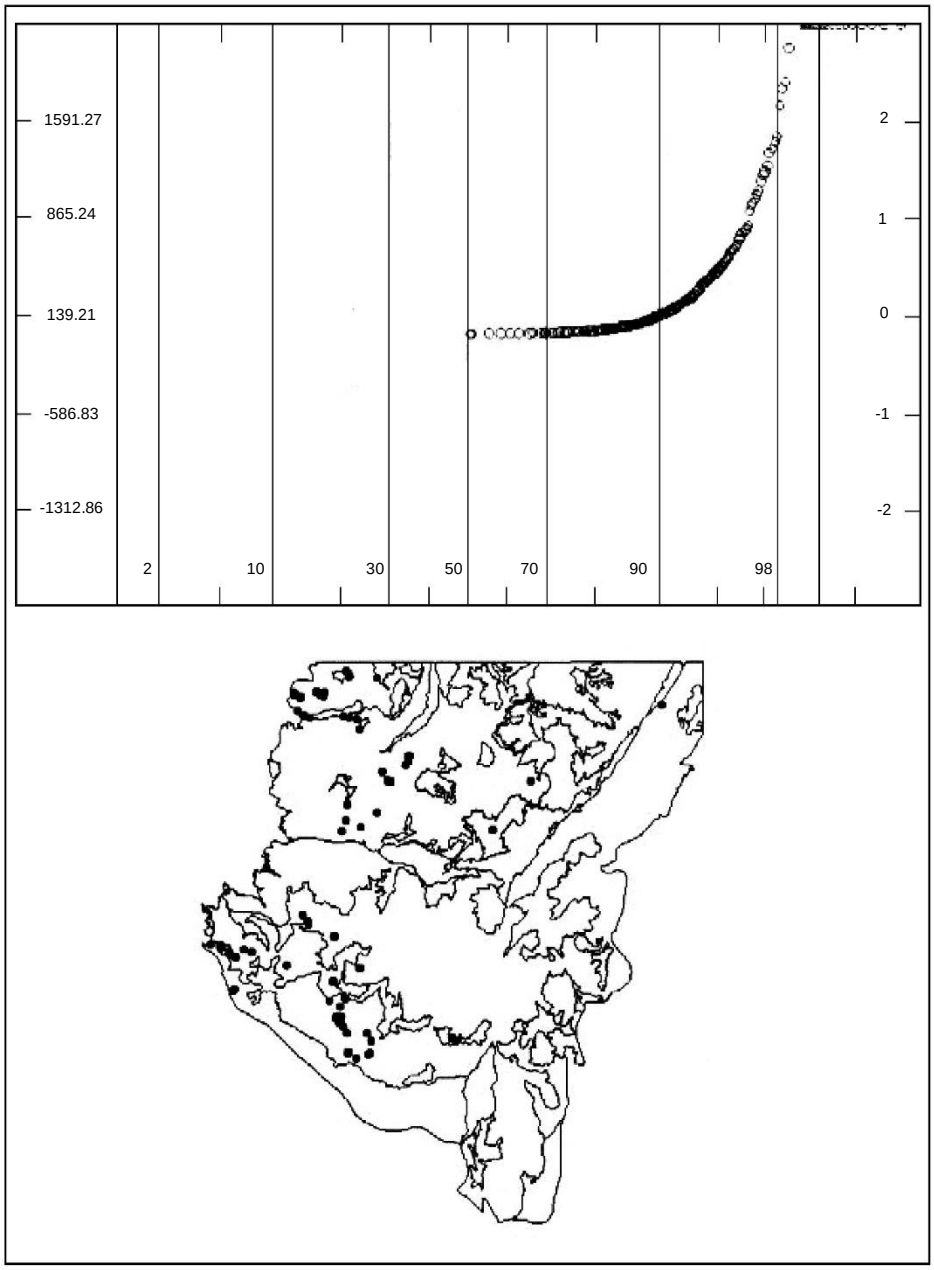

Figure 5. Cumulative probability plot and anomaly distribution for Au

Table 7. Metamorphic basement. Summary statistics

	Count	Mean	Std. Dev	Min	Max	Median
Au	347	43.82	156.97	3.33	1835	6
Ag	347	0.76	1.06	0.66	17.8	0.66
Cu	347	36.32	61.13	3	931	28
Pb	347	22.17	17.2	2.66	145	19
Zn	347	89.14	36.89	3.33	379.69	82
Mo	347	1.84	1.37	0.9	10	0.9
Ni	347	30.31	62.24	2.2	850.5	20
Co	347	14.82	7.27	1.73	70	13
Cd	347	0.56	0.27	0.46	2.5	0.46
Bi	347	4.3	1.72	4	32.5	4
Fe	347	3.59	1.1	0.55	9.07	3.47
Mn	347	687.87	292.83	63	2023	654
Te	347	6.75	1.07	6.66	23	6.66
Ba	347	119.01	49.24	21	308	113
Cr	347	47.04	57.2	2.46	854.5	35
V	347	66.47	32.17	2	292	62
Sn	347	13.55	1.96	13.33	38	13.33
W	347	13.57	1.6	13.33	28	13.33
La	347	16.33	9.71	0.66	67	14
Al	347	2.74	0.93	0.23	5.07	2.66
Mg	347	0.8	0.39	0.01	3.55	0.77
Ca	347	0.35	0.41	0.01	6.69	0.29
Na	347	0.02	0.01	0.01	0.09	0.02
K	347	0.2	0.15	0.03	1.14	0.16
Sr	347	25.41	20.79	-1	210	21
Y	347	8.44	3.19	2	23	8
Ga	347	4.25	3.06	1.33	15	4
Li	347	21.28	8.87	0.8	61	21
Nb	347	2.61	2.4	0.66	17	2
Sc	347	5.39	2.47	3.33	24	5
Ta	347	6.74	0.97	6.66	23	6.66
Ti	347	0.07	0.04	0.01	0.21	0.07
Zr	347	1.18	1.32	0.66	13	0.66
As	347	29.8	161.63	2.66	2880.95	11.5
Sb	347	2.2	2.8	1.26	36.25	1.26
Hg	347	0.09	0.31	0.03	4.91	0.05

Table 8. Pallatanga Unit. Summary statistics

	Count	Mean	Std. Dev	Min	Max	Median
Au	86	819.46	1857.09	3.33	9351	110
Ag	86	1.46	2.89	0.66	17.3	0.66
Cu	86	370.53	869.32	11	4799	112
Pb	86	65.81	259.18	2.66	1832	12
Zn	86	125.67	178.09	18	1023.5	83.5
Mo	86	1.9	1.54	0.9	8	0.9
Ni	86	82.86	71.72	5	393.06	70
Co	86	46.93	66.4	4.72	462.04	36
Cd	86	2.46	11.24	0.46	101	0.46
Bi	86	9.56	16.95	4	105	4
Fe	86	6.57	2.25	1.14	10*	7.04
Mn	86	982.53	519.08	187	2633	939
Te	86	9.75	11.09	6.66	77	6.66
Ba	86	70.54	45.78	5	250	66
Cr	86	131.27	86.21	14	433	122
V	86	174.79	68.49	19	297.5	186.75
Sn	86	13.72	2.13	13.33	29	13.33
W	86	13.65	2.09	13.33	29	13.33
La	86	7.51	6.52	0.66	39	6
Al	86	3.44	1.22	0.53	5.68	3.46
Mg	86	1.35	0.69	0.22	4.02	1.29
Ca	86	0.7	0.63	0.16	4.2	0.62
Na	86	0.02	0.02	0.01	0.14	0.02
K	86	0.07	0.05	0.01	0.26	0.05
Sr	86	18.62	9.52	-1	59	19
Y	86	7.81	4.16	2	22	7
Ga	86	5.52	3.89	1.33	14	5
Li	86	9.91	4.91	3	34	9
Nb	86	2.92	3.35	0.66	18	1.92
Sc	86	14.56	8.81	3.33	36	15
Ta	86	6.87	1.98	6.66	25	6.66
Ti	86	0.15	0.08	0.01	0.38	0.16
Zr	86	4.35	3.66	0.66	16.5	4
As	86	591	2021.01	2.66	10000*	23.65
Sb	86	12.66	42.37	1.26	306.6	2.13
Hg	86	0.9	4.04	0.03	33.84	0.1

*corresponds to the upper analytical reporting limit

Table 9. Celica Unit. Summary statistics

	Count	Mean	Std. Dev	Min	Max	Median
Au	27	49.714	115.557	3.33	535	7
Ag	27	0.66	0	0.66	0.66	0.66
Cu	27	29.167	11.518	3	63.5	28
Pb	27	39.21	25.628	2.66	102.5	32
Zn	27	142.021	78.209	3.33	328.9	134
Mo	27	2.198	1.225	0.9	5	2
Ni	27	10.7	6.449	2.2	28.5	9
Co	27	16.434	4.709	1.73	24	17
Cd	27	0.773	0.403	0.46	2.1	0.7
Bi	27	4.414	1.128	4	9	4
Fe	27	5.055	1.452	0.57	7.48	5.51
Mn	27	1088	473.138	235	2382.5	998
Te	27	6.66	0	6.66	6.66	6.66
Ba	27	101.111	35.749	22	206	102
Cr	27	20.813	9.906	2.46	42	20
V	27	97.815	47.071	9	231	97
Sn	27	13.33	0	13.33	13.33	13.33
W	27	13.33	0	13.33	13.33	13.33
La	27	12.358	6.154	0.66	28	11
Al	27	3.328	1.096	0.19	5.14	3.46
Mg	27	0.678	0.243	0.02	1.1	0.66
Ca	27	0.734	1.825	0.12	9.83	0.36
Na	27	0.018	0.009	0.007	0.05	0.02
K	27	0.098	0.056	0.007	0.27	0.08
Sr	27	30.228	21.481	-1	108	29
Y	27	9.537	4.842	2	23	9
Ga	27	6.067	3.316	1.33	13	6
Li	27	18	9.314	2	38	16.5
Nb	27	3.034	3.806	0.66	15	1
Sc	27	6.913	2.749	3.33	11.5	7
Ta	27	6.821	0.835	6.66	11	6.66
Ti	27	0.058	0.031	0.007	0.11	0.06
Zr	27	1.947	2.003	0.66	8.5	0.66
As	27	73.019	61.507	14.2	259.85	61.8
Sb	27	7.067	4.232	1.26	19.8	6.6
Hg	27	0.093	0.139	0.026	0.778	0.058

Table 10. Sacapalca Unit. Summary statistics

	Count	Mean	Std. Dev	Min	Max	Median
Au	250	16.61	43	3.33	416	3.33
Ag	250	0.68	0.18	0.66	3	0.66
Cu	250	30.9	45.44	3	419	21
Pb	250	26.44	102.73	2.66	1587.5	14
Zn	250	110.77	230.13	3.33	3643.5	87
Mo	250	2.19	2.35	0.9	26	0.9
Ni	250	9.84	6.76	2.2	50	8
Co	250	13.02	4.87	1.73	51	13
Cd	250	0.7	1.65	0.46	25.5	0.46
Bi	250	4.21	1.06	4	15	4
Fe	250	4.34	1.47	0.33	9.99	4.28
Mn	250	993.48	386.53	69	3351	958.5
Te	250	7.04	2.76	6.66	40	6.66
Ba	250	162.04	106.4	6	792	132.5
Cr	250	23.91	14.9	2.46	126	20
V	250	110.83	61.12	5	542	103.5
Sn	250	13.37	0.67	13.33	24	13.33
W	250	13.33	0	13.33	13.33	13.33
La	250	11.76	6.13	0.66	35	11.25
Al	250	2.8	0.92	0.21	6.36	2.78
Mg	250	0.75	0.3	0.01	1.56	0.74
Ca	250	1.21	1.08	0.02	7.57	0.86
Na	250	0.05	0.05	0.01	0.29	0.04
K	250	0.12	0.06	0.01	0.42	0.11
Sr	250	70.5	55.47	-1	285	60.5
Y	250	8.94	3.72	0.66	35	8.75
Ga	250	5.31	3.43	1.33	23	5
Li	250	11.93	6.73	0.8	40	10.5
Nb	250	2.81	3.45	0.66	24	0.66
Sc	250	6.67	2.45	3.33	15	7
Ta	250	7.03	3.49	6.66	56	6.66
Ti	250	0.11	0.08	0.01	0.47	0.1
Zr	250	6.08	4.61	0.66	27	5
As	250	17.83	26.56	2.66	238.6	9.93
Sb	250	2.29	3.17	1.26	37.65	1.26
Hg	250	0.08	0.1	0.03	0.89	0.04

Table 11. Saraguro Group. Summary statistics

	Count	Mean	Std. Dev	Min	Max	Median
Au	1134	145.42	766.43	3.33	10000.00*	3.33
Ag	1134	1.36	4.98	0.66	87.00	0.66
Cu	1134	145.57	1113.04	3.00	20000.00*	15.00
Pb	1134	44.97	238.17	2.66	6732.00	18.00
Zn	1134	124.19	363.17	3.33	8516.00	76.00
Mo	1134	15.74	198.39	0.90	4458.00	0.90
Ni	1134	9.17	9.74	2.20	119.44	7.00
Co	1134	12.14	7.46	1.73	64.82	11.00
Cd	1134	0.96	3.70	0.46	101.30	0.46
Bi	1134	5.12	6.88	4.00	121.50	4.00
Fe	1134	3.73	1.58	0.56	10.00*	3.63
Mn	1134	838.25	488.09	109.00	11890.00	772.00
Te	1134	6.75	1.25	6.66	44.00	6.66
Ba	1134	179.67	109.61	7.00	1333.00	153.00
Cr	1134	23.30	21.39	2.46	191.00	18.00
V	1134	79.28	50.68	5.00	382.00	69.00
Sn	1134	13.38	0.65	13.33	24.00	13.33
W	1134	15.66	39.80	13.33	844.50	13.33
La	1134	11.92	6.95	0.66	103.00	11.00
Al	1134	2.94	1.06	0.19	6.68	2.86
Mg	1134	0.56	0.34	0.02	1.90	0.53
Ca	1134	0.47	0.43	0.03	7.62	0.39
Na	1134	0.02	0.03	0.01	0.33	0.02
K	1134	0.11	0.07	0.01	0.58	0.09
Sr	1134	41.71	36.33	-1.00	290.00	32.00
Y	1134	7.22	3.03	1.00	25.00	7.00
Ga	1134	5.04	3.49	1.33	32.17	5.00
Li	1134	12.14	7.55	0.80	58.00	11.00
Nb	1134	2.11	2.29	0.66	19.00	1.00
Sc	1134	5.31	2.56	3.33	29.00	3.33
Ta	1134	6.75	1.78	6.66	62.00	6.66
Ti	1134	0.07	0.06	0.01	0.58	0.06
Zr	1134	3.46	3.50	0.66	26.00	2.00
As	1134	44.15	165.25	2.66	3176.60	11.80
Sb	1134	6.28	63.52	1.26	2000.00*	1.26
Hg	1134	0.23	1.69	0.03	50.00*	0.06

*corresponds to the upper analytical reporting limit

Table 12. Ayancay Group. Summary statistics

	Count	Mean	Std. Dev	Min	Max	Median
Au	138	33.975	134.506	3.33	1045	3.33
Ag	138	0.67	0.083	0.66	1.4	0.66
Cu	138	19.946	10.893	3	116	18
Pb	138	14.293	10.302	2.66	102	12.5
Zn	138	90.404	37.644	30	209	82
Mo	138	1.492	0.976	0.9	5	0.9
Ni	138	9.188	6.241	2.2	62	8
Co	138	13.803	5.857	1.73	41	13
Cd	138	0.481	0.137	0.46	1.95	0.46
Bi	138	4.203	1.215	4	17	4
Fe	138	4.408	1.88	1.23	10	3.985
Mn	138	893.42	293.865	41	2127	864.5
Te	138	6.892	1.592	6.66	23	6.66
Ba	138	173.812	86.863	3.6	678.5	157
Cr	138	20.691	14.158	2.46	83.5	16
V	138	149.804	112.964	2	747.5	114
Sn	138	13.47	1.185	13.33	25	13.33
W	138	13.407	0.908	13.33	24	13.33
La	138	9.083	4.018	0.66	32	9
Al	138	2.785	0.96	0.24	6.4	2.585
Mg	138	0.802	0.364	0.007	1.75	0.818
Ca	138	1.148	1.127	0.02	10	0.895
Na	138	0.083	0.069	0.007	0.4	0.065
K	138	0.093	0.05	0.03	0.3	0.08
Sr	138	98.986	51.086	-1	308	93.5
Y	138	6.19	2.105	0.66	14	6
Ga	138	3.46	2.76	1.33	13	2
Li	138	9.705	6.292	0.8	31	7.25
Nb	138	1.775	2.063	0.66	15	0.66
Sc	138	5.939	1.828	3.33	11	6
Ta	138	6.66	0	6.66	6.66	6.66
Ti	138	0.124	0.093	0.007	0.435	0.11
Zr	138	7.191	4.144	0.66	23	7
As	138	15.449	21.885	2.66	173.6	8.2
Sb	138	1.582	1.277	1.26	11	1.26
Hg	138	0.094	0.237	0.026	2.644	0.05

Table 13. Quimsacocha Formation. Summary statistics

	Count	Mean	Std. Dev	Min	Max	Median
Au	13	5.36	2.78	3.33	10	3.33
Ag	13	0.66	0	0.66	0.66	0.66
Cu	13	12.38	2.72	8	18	12
Pb	13	13.35	5.05	5	25	14
Zn	13	84.61	34.64	32	154	83
Mo	13	1.55	0.81	0.9	3	0.9
Ni	13	3.75	1.7	2.2	7	3.5
Co	13	12.49	9.84	5	43	10
Cd	13	0.48	0.07	0.46	0.7	0.46
Bi	13	4	0	4	4	4
Fe	13	2.97	0.73	1.92	4.7	3.04
Mn	13	1164.81	913.9	187	3646	1053
Te	13	6.66	0	6.66	6.66	6.66
Ba	13	198.35	84.58	107	428	177
Cr	13	8.46	3.13	2.46	13	10
V	13	85.35	23.61	49	122	83
Sn	13	13.33	0	13.33	13.33	13.33
W	13	13.33	0	13.33	13.33	13.33
La	13	6.09	3.5	0.66	15	5
Al	13	3.18	1.3	1.88	5.39	2.57
Mg	13	0.17	0.1	0.02	0.36	0.17
Ca	13	0.35	0.22	0.09	0.96	0.29
Na	13	0.03	0.03	0.01	0.11	0.02
K	13	0.03	0.01	0.01	0.05	0.03
Sr	13	74.77	37.48	-1	137	75
Y	13	3.08	1.32	1	6	3
Ga	13	6.44	6.69	1.33	21	3
Li	13	6.23	4.17	3	17	5
Nb	13	1.15	0.9	0.66	3	0.66
Sc	13	3.59	0.63	3.33	5	3.33
Ta	13	6.66	0	6.66	6.66	6.66
Ti	13	0.15	0.07	0.07	0.35	0.14
Zr	13	5.88	5.4	2	21	5
As	13	11.31	17.77	2.66	63.2	2.66
Sb	13	1.26	0	1.26	1.26	1.26
Hg	13	0.1	0.12	0.03	0.36	0.05

Table 14. Turi Formation. Summary statistics

	Count	Mean	Std. Dev	Min	Max	Median
Au	75	5.02	4.98	3.33	37	3.33
Ag	75	0.7	0.2	0.66	2.1	0.66
Cu	75	18.06	8.63	3	42	15
Pb	75	17.83	11.07	6	66	15
Zn	75	99.94	43.95	52	284.5	87
Mo	75	1.59	1.41	0.9	9	0.9
Ni	75	6.2	3.48	2.2	17	5
Co	75	10.66	3.82	1.73	27	10
Cd	75	0.49	0.2	0.46	2	0.46
Bi	75	4.04	0.35	4	7	4
Fe	75	3.79	1.32	2.14	8.92	3.29
Mn	75	635.63	301.09	113	1591	564
Te	75	6.66	0	6.66	6.66	6.66
Ba	75	172.76	77.81	13	538	155.5
Cr	75	12.55	6.88	2.46	37	11
V	75	125.73	58.06	35	379	112
Sn	75	13.33	0	13.33	13.33	13.33
W	75	13.74	2.05	13.33	25	13.33
La	75	7.78	3.13	0.66	15	7
Al	75	3.63	2.11	0.89	9.48	2.96
Mg	75	0.31	0.33	0.03	1.26	0.15
Ca	75	0.4	0.3	0.06	1.74	0.36
Na	75	0.03	0.03	0.01	0.13	0.02
K	75	0.04	0.02	0.02	0.18	0.04
Sr	75	70.9	34.29	-1	203	70
Y	75	3.72	1.91	1	13	3
Ga	75	6.46	6.41	1.33	30	4
Li	75	5.86	4.95	1.5	32	5
Nb	75	0.92	0.65	0.66	4	0.66
Sc	75	4.32	1.46	3.33	8	3.33
Ta	75	6.66	0	6.66	6.66	6.66
Ti	75	0.17	0.09	0.01	0.41	0.17
Zr	75	11.78	8.11	0.66	37	10
As	75	22.09	112.57	2.66	973.15	4.3
Sb	75	1.5	0.94	1.26	8.2	1.26
Hg	75	1.91	8.29	0.03	50*	0.06

*corresponds to the upper analytical reporting limit

Table 15. Tarqui Formation. Summary statistics

	Count	Mean	Std. Dev	Min	Max	Median
Au	17	5.37	5.1	3.33	23	3.33
Ag	17	0.66	0	0.66	0.66	0.66
Cu	17	13.24	6.34	6	34	13
Pb	17	8.69	3.64	2.66	17	9
Zn	17	59.35	17.22	37	97	54
Mo	17	1.4	0.92	0.9	4	0.9
Ni	17	4.62	5.22	2.2	24	4
Co	17	8.88	4.69	3	22	9
Cd	17	0.48	0.08	0.46	0.8	0.46
Bi	17	4	0	4	4	4
Fe	17	2.66	0.8	1.46	4.61	2.68
Mn	17	756.53	706.48	92	3101	506
Te	17	6.66	0	6.66	6.66	6.66
Ba	17	189.29	72.6	88	330	179
Cr	17	8.67	7.79	2.46	37	8
V	17	62.88	20.3	31	98	70
Sn	17	13.33	0	13.33	13.33	13.33
W	17	13.33	0	13.33	13.33	13.33
La	17	7.76	4.49	0.66	14	8
Al	17	2.08	0.76	1.03	4.1	2.08
Mg	17	0.37	0.38	0.09	1.69	0.23
Ca	17	0.48	0.38	0.08	1.5	0.45
Na	17	0.04	0.03	0.01	0.15	0.03
K	17	0.1	0.04	0.05	0.19	0.09
Sr	17	44.24	36.53	-1	131	34
Y	17	4.53	2.12	1	8	4
Ga	17	4.31	2.51	1.33	10	4
Li	17	6.29	3.67	2	15	5
Nb	17	1.53	1.55	0.66	6	0.66
Sc	17	3.82	1.48	3.33	9	3.33
Ta	17	6.66	0	6.66	6.66	6.66
Ti	17	0.08	0.06	0.01	0.18	0.07
Zr	17	4.78	3.92	0.66	13	4
As	17	154.81	581.36	2.66	2407.4	5
Sb	17	1.51	0.62	1.26	3.5	1.26
Hg	17	0.05	0.03	0.03	0.12	0.05

Table 16. Major granodiorite and diorite intrusions. Summary statistics

	Count	Mean	Std. Dev	Min	Max	Median
Au	299	152.69	608.71	3.33	6878	15
Ag	299	0.98	3.22	0.66	54.3	0.66
Cu	299	89.9	586.78	3	10000*	36
Pb	299	62.1	268.93	2.66	4210.5	23
Zn	299	154.84	406.19	19	5727	92
Mo	299	2.71	3.42	0.9	43.83	2
Ni	299	13.59	10.24	2.2	119.44	11
Co	299	15.05	9.97	5	154	14
Cd	299	1.68	8.38	0.46	137.1	0.46
Bi	299	5.56	12	4	203.5	4
Fe	299	4.76	1.74	1.62	10*	4.48
Mn	299	810.37	396.42	120	2882	758
Te	299	7.68	10.04	6.66	169.5	6.66
Ba	299	119.27	47.36	3.5	337	113
Cr	299	35.43	25.74	5	174	31
V	299	114.06	71.55	18	720	94
Sn	299	13.88	3.84	13.33	56	13.33
W	299	13.7	3.01	13.33	55	13.33
La	299	10.25	6.55	0.66	40	9
Al	299	3.1	1.12	0.55	7.7	3.01
Mg	299	0.79	0.27	0.09	1.86	0.79
Ca	299	0.51	0.6	0.05	4.18	0.37
Na	299	0.02	0.01	0.01	0.08	0.02
K	299	0.14	0.09	0.02	0.68	0.12
Sr	299	26.8	17.47	-1	123	25
Y	299	7.77	3.77	2	23	7
Ga	299	5.7	3.68	1.33	36	5
Li	299	15.01	6.74	0.8	43	14
Nb	299	2.95	4.34	0.66	51	1.33
Sc	299	5.51	2.62	3.33	18	5
Ta	299	7.76	9.45	6.66	146.33	6.66
Ti	299	0.09	0.04	0.01	0.21	0.09
Zr	299	1.65	1.86	0.66	16	0.66
As	299	127.64	745.24	2.66	10000*	18.6
Sb	299	4.75	14.66	1.26	175.9	2
Hg	299	0.15	0.45	0.03	5.53	0.06

*corresponds to the upper analytical reporting limit

5.3.4 Arsenic and antimony

Arsenic and antimony are closely covariant throughout the 3°-4°S quadrangle (Table 6). Their distributions may thus conveniently be described simultaneously. While ratios vary in accordance with temperature, both elements form important components of epithermal and mesothermal assemblages in the Bella Rica-San Gerardo and Zaruma-Portovelo fields, and in occurrences north of the Jubones Fault between La Playa and Tres Chorreras.

Cumulative probability data for As and Sb (Figs. 6-7) depict thresholds for the entire population at 68 mg/kg (90th %ile) and 4 mg/kg (91st %ile) respectively. Strongly anomalous values exceed 451 mg/kg (98th %ile) and 21 mg/kg (98th %ile) respectively. Background metalloid abundances display marked lithostratigraphic variation. If mineralised localities are excluded, highest median abundances prevail over intermediate and mafic lithologies of the Pallatanga Unit (>20 mg/kg As), the Celica Unit (>30 mg/kg As), the Portovelo Unit (>20 mg/kg As) and the undifferentiated Saraguro Group west of the Jubones Caldera. Systematically lower As backgrounds characterise dacitic and rhyolitic Saraguro Group facies in the east of the mapped area.

A significant multi-sample As anomaly is recorded over the basement inlier at Dumari in association with documented polymetallic vein mineralisation. Examples include sites 976 [ref. 642731-9618224], 417 [ref. 642322-9618343] and 483 [643823-9619014], with values of As to 369 mg/kg, Sb to 32 mg/kg, Cu to 167 mg/kg, Pb to 207 mg/kg and Au to 1454 μg/kg. Other basement anomalies, generally coincident with Au (5.3.3 above) occur in the Santa Rosa basin (site 2691, ref. 629054-9603631; site 3528, ref. 628644-9603334) where As values to 2880 mg/kg are recorded, and in the alluvial fill of the Río Palenque south of the Jubones Fault.

Over the Pallatanga Unit anomalous As and Sb values, typically associated with Au, occur in four discrete catchment areas. In the Río Siete (draining southward from Bella Rica) As values in the range 245-10000 mg/kg occur with up to 237 mg/kg Sb at sites 390 [ref. 641748-9658777], 484 [ref. 642230-9658397], 938 [ref. 642663-9657973] and 101 [ref. 644027-9657490]. Values of Cu to 9012 mg/kg are recorded at these stations. Close to Ponce Enríquez, the lower Estero Guanache yields several high values attributable to sediment outwash from both Bella Rica and Gaby. Examples include site 744 [ref. 642324-9661716], in which 10000 mg/kg As occurs with 113 mg/kg Sb, 9631 μg/kg Au, 4624 mg/kg Cu and 1832 g/kg Pb. This mesothermal (high As/Sb, base-metal rich) signature grades to one characteristic of a lower temperature assemblage in the Río Tenguel and Río Chico systems. In the former, site 278 [ref. 646329-9662001] is one of four strongly anomalous stations with respect to As. In the San Gerardo zone, higher Sb contents and lower base metal concentrations are more pronounced, for example at site 894 [ref. 651461-9666603] which yields 5094 mg/kg As and 306 mg/kg Sb with very low abundances of Cu, Pb and Zn.

Over the Saraguro Group, the Portovelo Unit of the Zaruma-Portovelo field is highlighted by a succession of As anomalies in the south-trending Río Bono-Río Calera system. The northern limit of this zone encompasses south-flowing drainage from a diorite source east of breccia pipe occurrences at Paccha (site 5510, ref. 651008-9601947). Here, a value of 3176 mg/kg As occurs with 43 mg/kg Sb, 3 mg/kg Hg, 1263 μg/kg Au, 4996 mg/kg Cu, 1834 mg/kg Pb, 4309 mg/kg Zn, 27 mg/kg Cd and 53 mg/kg Bi. Río Bono anomalies, sourced from documented mesothermal polymetallic lodes, occur at sites 3481 [ref. 650391-9600266] and 2439 [ref. 650183-9597101] with As values of 890-1239 mg/kg As accompanied by strong Au-Cu-Pb enrichment. The Río Calera close to the contact of the Portovelo Unit and the Zaruma rhyolite, yields As values to ca. 500 mg/kg, with Cu to 8598 mg/kg and Pb to 6732 mg/kg (e.g. site 3258, ref. 650838-9596194). This base-metal rich signature prevails despite increasing epithermal overprinting in this area. Southwest of Zaruma, a value of 347 mg/kg As with 46 mg/kg Sb is recorded at site 3164 [ref. 651822-9591028], marking the southern limit of the strongly anomalous zone.

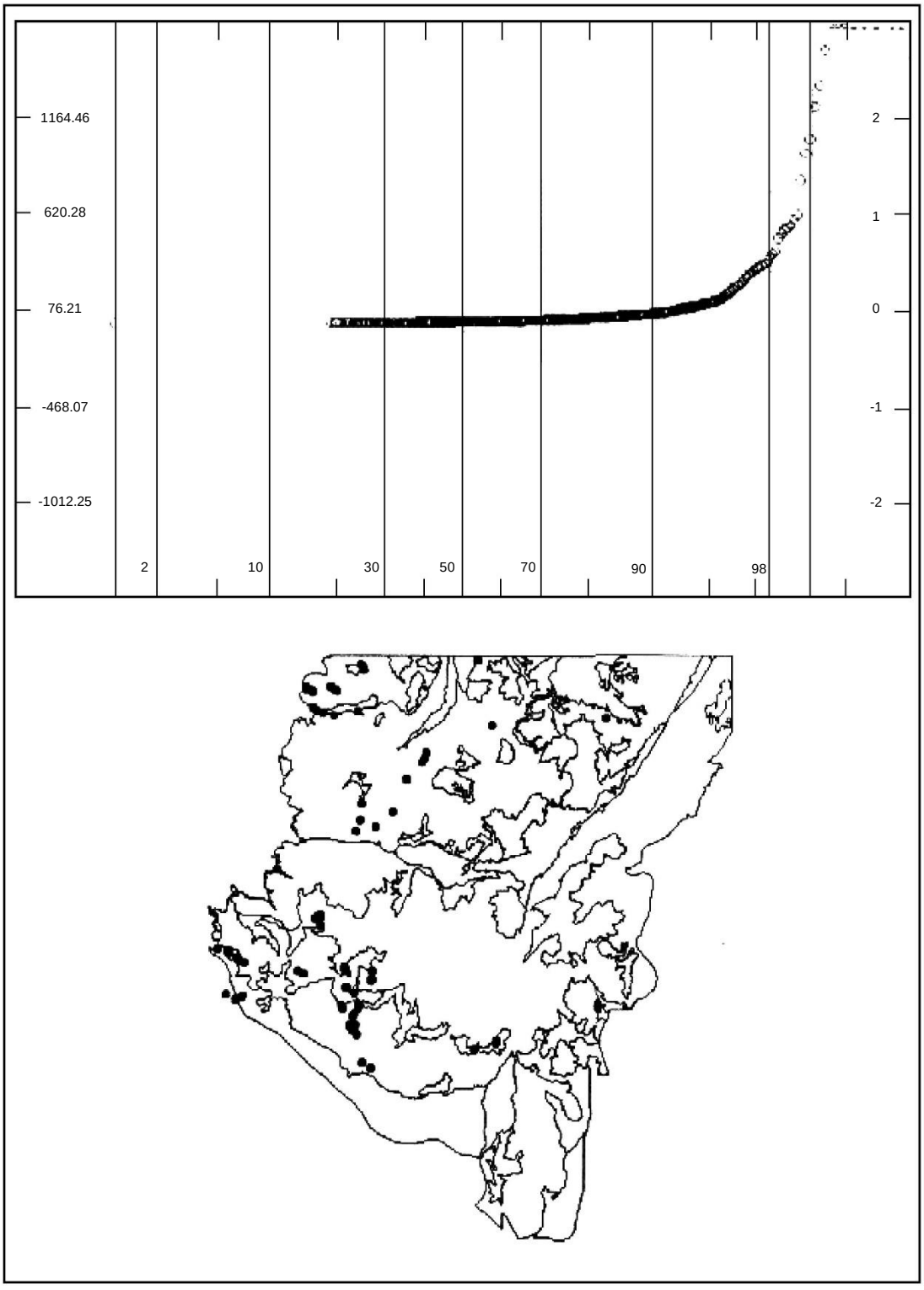

Figure 6. Cumulative probability plot and anomaly distribution for As

North of the Jubones Fault, all conspicuous As and Sb anomalies relate to documented mines and prospects. At Tres Chorreras, site 1714 [ref. 663959-9649821] yields 2388 mg/kg As, 2000 mg/kg Sb, 2622 mg/kg Mo and 3634 mg/kg Cu. An anomaly within the Río San Martín (ref. 659775-9645029, 257 mg/kg As, 144 mg/kg Sb) highlights La Enramada. Low As/Sb ratios are characteristic of both localities. The La Playa and La Tigrera mine areas are characterised by modest As anomalies (to 500 mg/kg) within a Cu-Mo-W rich assemblage (e.g. site 303, ref. 651549-9640288). South of La Playa, other minor intrusions control As-rich polymetallic mineralisation, notably close to Mollepungu (site 340, ref. 651435-9637102).

Elevated As values to 305 mg/kg are recorded in south-east flowing tributaries of the Río Ramos (e.g. site 2106 ref. 767773-9655191) in association with an outcrop of andesite porphyry in the Saraguro Group tract north-west of Shagli. Such values may, in part, be lithological, although argillic alteration and an abundance of disseminated sulphide is locally prevalent.

The predominantly low-sulphidation epithermal prospects of the central and northern Gañarín Belt produce a poor response with respect to As. An exception occurs 2 km north-east of the Cañaribamba prospect, where a south-east flowing tributary of the Río Naranjo cuts a diorite stock, yielding 81 mg/kg As with 3046 μg/kg Au. Locally intense alteration of the Saraguro Group is recorded close to the intrusive contact.

Post Saraguro Group volcanic and sedimentary sequences yield high As values in the north-east of the mapped area, notably at the eastern margin of the Quimsacocha Caldera, at the contact of the rhyolitic core and sediments of the Turi Formation (site 1273, ref. 698871-9663942, 245 mg/kg As, 9.7 mg/kg Sb, 611 mg/kg Cu, 0.57 mg/kg Hg). To the south of the Quimsacocha lava pile, 973 mg/kg As is recorded over the Turi Formation in the Río Cristal system. The Tarqui Formation of the Saraguro area hosts two anomalous As values to 2400 mg/kg in tributaries of the R. Paquishapa at the contact with andesites of the Sacapalca Unit. No attendant enrichment of elements of economic interest is recorded. A travertine mine is located 0.5 km to the north.

Conspicuous As anomalies over intrusive terranes are confined to three localities. East of Santa Rosa, values in Q. Las Moras (site 2820, ref. 626196-9612056) and Río Byron (e.g. site 5676, ref. 628103-961031) reach 5838 mg/kg As with 34 mg/kg Sb, 3747 μg/kg Au, 1616 mg/kg Cu and 468 mg/kg Pb. These probably reflect alluvial outwash from the Cerro Pelado mine area, 5 km to the south, where mesothermal veins associated with tourmaline breccias are hosted by rhyodacitic volcanic facies. Near Paccha, site 3714 [ref. 648821-9605120] in a tributary of the Río Higuerillas yields 10000 mg/kg As and 168 mg/kg Sb as components of a highly Au-Cu-Cd rich assemblage. Extensive hydrothermal alteration, disseminated sulphides and widespread hydrothermal brecciation with tourmaline cementation are reported. High Hg values at this locality are considered most likely to reflect contamination. Approximately 10 km north-west of Paccha, an As value of 1057 mg/kg with 1149 μg/kg Au and 368 mg/kg Pb occurs in an additional zone of tourmaline-rich breccias at site 6012 [ref. 639610-9608300]. Possible multi-phase mineralisation includes a suite of mesothermal veins carrying arsenopyrite and galena.

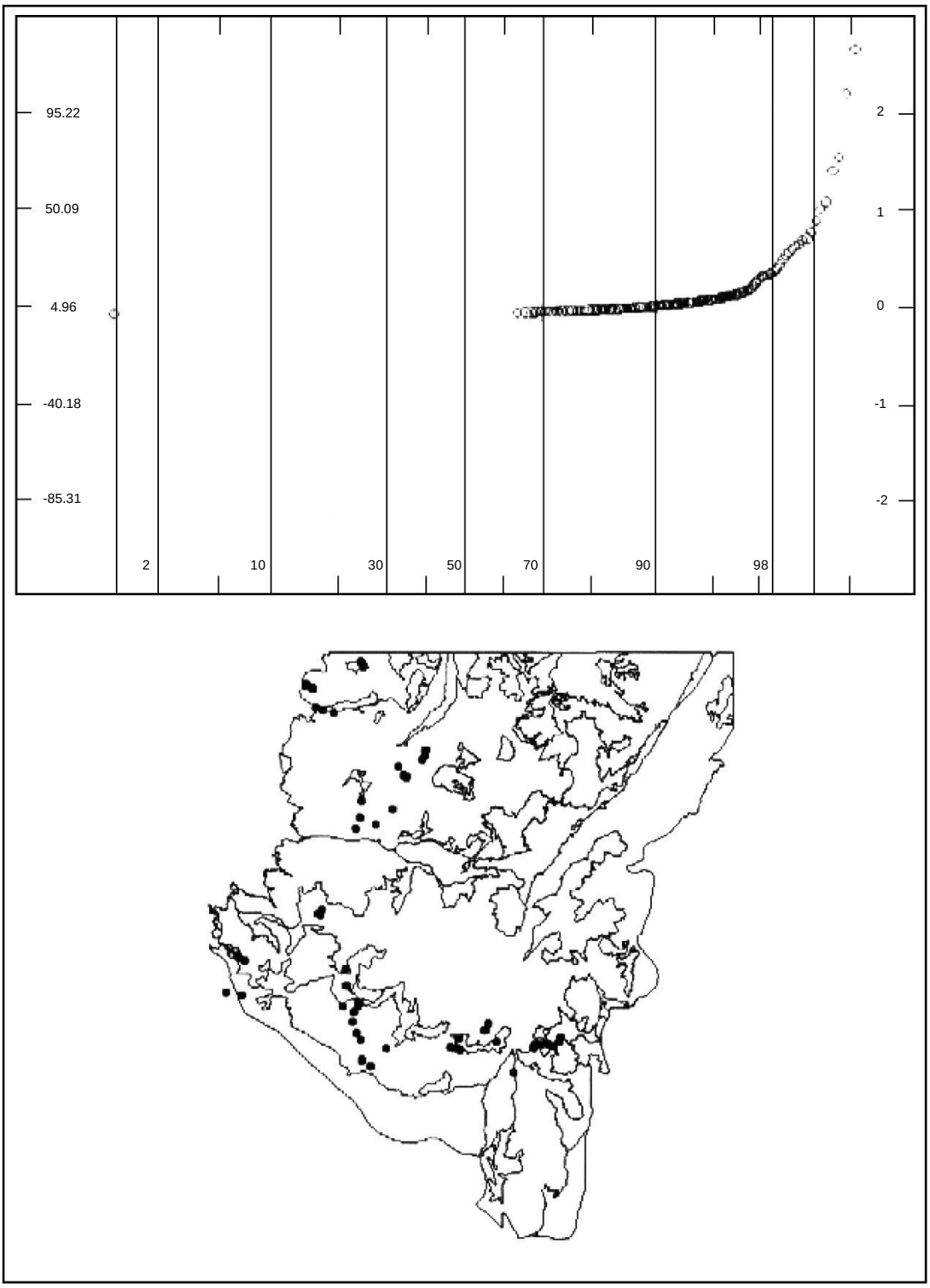

Figure 7. Cumulative probability plot and anomaly distribution for Sb

5.3.5 Mercury

Values of Hg in the range <0.03-0.2 mg/kg characterise 92% of the 3°-4°S dataset. Cumulative probability data (Fig. 8) illucidate a threshold at ca. 0.40 mg/kg, with strongly anomalous values in the range 2.1 – >50 mg/kg. Many such anomalous values occur within the mining districts of Ponce Enríquez-Bella Rica and Portovelo-Zamora. The close statistical correlation between Hg and Au in these districts is of little metallogenic significance, being primarily attributable to the anthropogenic release of Hg during Au beneficiation.

Basement rocks in the 3°-4°S area host few Hg values of significance. South the Jubones Fault, a value of 0.8 mg/kg Hg with coincident enrichment of Au (2391 μg/kg) and As (3701 mg/kg) is recorded in the alluvial fill of the Río Palenque basin (site 6609, ref. 635598-9627663).

Contaminant Hg enrichment is widely evident in the Bella Rica-San Gerardo tract of the Pallatanga Unit. The Río Guanache, partially draining both the Bella Rica and Gaby localities yields several values in the range 1-3.25 mg/kg, characteristically in Au-Cu-Cd-Zn-As rich assemblages (e.g. site 560, ref. 640320-9661491; site 30, ref. 641483-9661772; site 788, ref. 640875-9661820). Values of ca. 0.3-0.6 mg/kg Hg prevail in the NW-flowing Río Tenguel system (e.g. site 628, ref. 645424-9662716; site 278, ref. 646329-9662001). In the San Gerardo block, the Río Chico and NE-flowing tributaries yield values of 1.6-3.2 mg/kg Hg (e.g. site 894, ref. 651461-9666603; site 105, ref. 651467-9666223; site 803, ref. 651951-9665667), with coincident enrichment of Au to 8675 μg/kg and As to 6138 mg/kg.

East of the Bella Rica tract an elongate tongue of the Pallatanga Unit bounded to the east by Q. Mangán hosts strongly anomalous Hg values in the range 2.3-33.8 mg/kg within the NE-trending Río Chiguay (site 5254, ref. 665304-9655593; site 2448, ref. 665690-9656201; site 6551, ref. 665997-9656993). No attendant Au, base metal or metalloid enrichment is recorded. Tectonic (possibly hydrothermal) breccias occur 1-2 km to the south.

Over the Saraguro Group, an elevated Hg background prevails over the Zaruma-Portovelo block as a probable function of artisanal mining impacts. West of the contact of the Portovelo Unit and the Undifferentiated Saraguro Group, a Hg value of 1.2 mg/kg is recorded in Q. El Trigal (site 5270, ref. 650697-9593601), an east-trending tributary of Río La Calera. Approximately 1.5 km north-east of Portovelo (site 6347, ref. 653489-9590121) a value of 0.85 mg/kg Hg with 1888 μg/kg Au, 385 mg/kg As and attendant base-metal enrichment occurs close to a minor rhyolite stock or dome. A more striking anomaly of >50 mg/kg Hg with 6789 μg/kg Au occurs in Q. Honda (site 6227, ref. 655585-9594969), a south-flowing tributary of the Río Amarillo system.

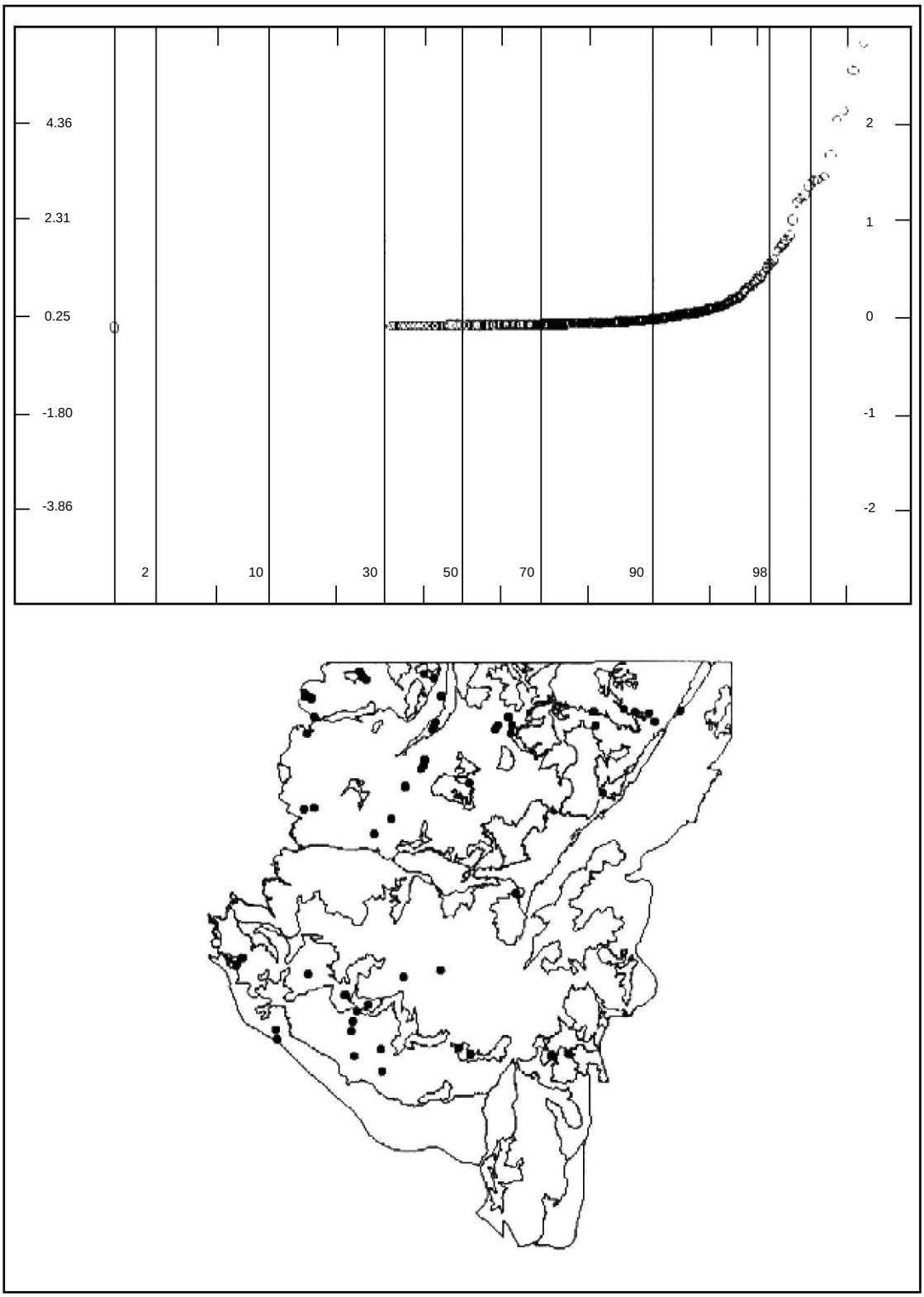

Figure 8. Cumulative probability plot and anomaly distribution for Hg

In the central sector of the 3°-4°S area a pronounced Hg anomaly of 14.64 mg/kg, with no attendant Au or base metal enrichment, occurs within the Río San José fault zone on the southern margin of the Cordillera de Corredores (site 6979, ref. 666963-9608906). Silicified rhyolitic tuffs to the west show disseminated pyrite. Further east, a value of 14.1 mg/kg Hg is recorded in Q. del Salado, an east-flowing tributary of the Río Manú-Río Uchucay system. Hydrothermally altered andesites occur to the south. The close proximity of a travertine operation indicates a possible (palaeo) hot-spring influence.

North of the Jubones Fault, the Tres Chorreras-La Playa tract of the Saraguro Group hosts numerous Hg anomalies, primarily of anthropogenic origin. At Tres Chorreras, sites 813 [ref. 663761-9649831] and 1714 [ref. 663959-9649821] yield Hg values in excess of 3 mg/kg with Au to 9561 μg/kg, As to 2388 mg/kg, Sb to 2000 mg/kg and W to 80 mg/kg. Río Gigantes sites 988 [ref. 663356-9648122] and 190 [ref. 660295-9644770] host Hg values of 1.9-4.4 mg/kg, with up to 7520 μg/kg Au, 53 mg/kg Ag, 20000 mg/kg Cu, 1495 mg/kg As, 88 mg/kg W, 664 mg/kg Pb and 4450 mg/kg Mo. The latter site is strongly influenced by the Gigantones Au workings 2 km to the NNW.

Within the postulated Jubones Caldera, an Hg value of 1.83 mg/kg occurs at the northern contact of tuffaceous volcanics with an exposed rhyolite core east of Pucará (site 1205, ref. 672448-9645419). Unaccompanied by Au, metalloid or base metal enrichment, this Hg enrichment may reflect a high-level expression of an epithermal system associated with resurgent sub-volcanic activity. Further north-west, three anomalous Hg values in the range 2.8-11.6 mg/kg occur in Q. Cordorcocha, a south-flowing tributary of the Río Minas. Values increase towards the headwaters. The distribution is antipathetic to Au. The most southerly Hg anomaly (site 2722, ref. 679901-9657905) occurs in a zone of intense silicification (of either Saraguro volcanics or chilled intrusive lithologies) with abundant disseminated sulphides. These anomalies may potentially reflect distant, low-temperature emanations associated with the Salvias and Shagli centres.

In the post-Saraguro tract, pronounced non-anthropogenic Hg enrichment is associated with the Quimsacocha eruptive centre. Extremely high values are orientated along the southern margin of the lava pile, notably along an elongate SE-trending tongue. Sites 1607 [ref. 701945-9659415], 1274 [ref. 704142-9658976] and 1842 [ref. 706812-9658715] yield 31.9 – >50 mg/kg Hg. Further west, over the fringing Tarqui Formation, values of 2.9-3.1 mg/kg are recorded. A systematic lack of attendant Au or base metal enrichment is consistent with trends along the northern margin of the Quimsacocha Formation, north of the 3°S line (Williams et al., 1997). GIMP reconnaissance data for sites closer to the rhyolitic core of the caldera are not available due to the lack of surface drainage. Field observations suggest, however, an increasing sulphide presence with abundant enargite and disseminated cinnabar. The Hg values reported are therefore interpreted as defining the outer (lowest temperature) limit of the Quimsacocha epithermal system.

5.3.6 Copper

The regional Cu distribution in the 3°-4°S quadrangle is subject to a strong lithological control. Highest backgrounds prevail over the Pallatanga Unit (median 100 mg/kg), the Celica Unit and the metamorphic basement. Lithological contrasts in the Saraguro Group are clearly discriminated, predominantly dacitic and rhyolitic facies to the north and east of Chilla yielding a systematically low background (<10 mg/kg) relative to andesitic composition to the south and west. Granodiorite and diorite intrusions in the southern sector of the quadrangle are relatively Cu-rich, with a median stream sediment values of ca. 50 mg/kg.

With the exception of the base-metal poor epithermal Au occurrences of the Gañarín Belt, anomalous Cu values are closely coincident with Au. Values within the uppermost 3 %ile of the population are thus recorded in drainage on the southern flank of the Bella Rica field (Río Siete), south-west of the Gaby porphyry (Río Estero Guanache), the Río Calera system in the Zaruma area, and breccia pipe and related mesothermal occurrences at Tres Chorreras, La Tigrera, Gigantones, Paccha and Cerro Pelado (see sections 5.3.3-5.3.5 for locational details and concentration data).

In addition to porphyry mineralisation at Gaby, porphyry and associated stockwork mineralisation associated with a granodiorite intrusion and later rhyolite stock at Fierro Urcu is highlighted by Cu values of 366-419 mg/kg at sites 2057 and 5943 (refs. 683267-9589008; 683898-9589427). Values of Au to 416 μg/kg are recorded in this locality. Concentrations of Mo and other base metals are typically low.

The presence of enargite within mineral assemblages at Quimsacocha is indicated by a value of 611 mg/kg Cu in the headwaters of Q. Quinuahuaycu at the eastern contact of the Quimsacocha rhyolite with the surrounding andesite lavas (site 1273, ref. 698871-9663942).

6. DISCUSSION AND CONCLUSIONS

6.1 Economic potential

6.1.1 Interpretive guidelines

The drainage reconnaissance dataset described provides a potentially valuable tool for economic evaluation of the 3°-4°S sector of the Cordillera Occidental, subject to the recognition of a number of constraints.

6.1.1.1 Resolution: At the resolution of sampling undertaken, significant mineral occurrences may be resolved by only a single anomalous sample. This is exemplified with respect to several known prospects including Paccha, Gañarín and Cañaribamba.

6.1.1.2 Terrain influence: High páramo sediment geochemical signatures are controlled by physical rather than hydromorphic processes and peak/background ratios, notably for transition metals, are thus low. This, coupled with the high energies characteristic of high páramo drainage, results in often subtle responses to mineralisation. At lower elevations, including the Zaruma and Ponce Enríquez areas, greater base-metal and metalloid mobility is prevalent and hydrous oxides exert a more significant control on the intensity of drainage anomalies. In addition to lithological normalization, such physiographic variations warrant consideration in data interpretation.

6.1.1.3 Style of mineralisation: While several mineral occurrences associated with mesothermal veins, tourmaline breccias, porphyries and exhalative massive sulphides are illucidated by strong base-metal and metalloid enrichment of sediment samples, many known epithermal occurrences of the Gañarín Belt produce an inconspicuous drainage response. It is thus probable that additional occurrences of analogous low-sulphidation (adularia) character are poorly resolved by the drainage reconnaissance methodology deployed.

6.1.1.4 Anthropogenic influence: Natural drainage responses to mineralisation are modified substantially by mining, mineral processing and the disposal of sub-ore grade wastes in many sectors of the 3°-4°S area. Precise derivation of the geological controls on drainage anomalies in the Bella Rica-Ponce Enríquez and Zaruma fields is effectively precluded.

6.1.2 Significance of geochemical anomalies

The 3°-4°S quadrangle hosts a diversity of metalliferous mineralisation unparalleled within the Cordillera Occidental. While most conspicuous geochemical anomalies (Table 17) relate to documented deposits (many of which support ongoing artisanal or medium-scale mining activities), potential exists for the identification of new prospects, particularly base-metal poor, low-temperature occurrences. Such deposits are inconspicuous both geochemically and in surface mineralogical expression, and are thus frequently overlooked by artisanal prospectors.

Table 17. Summary of principal drainage anomalies in the 3°-4°S sector of the Cordillera Occidental

No.	Terrain	Location	UTMX	UTMY	Au (ppb)	Element association	Setting
1	Basement	Dumari	6438	96190	to 1454	Pb-As-Sb-Cu	Mesothermal veins
2	Basement	Río Santa Rosa	6257	96039	to 1835	Cu-Bi-Ag-As-Sb	Unknown source
3	Pallatanga	Gaby**	6423	96617	to 9351	Ag-Cu-Pb-Bi-As-Sb	Porphyry and stockwork
4	Pallatanga	Bella Rica (south)	6417	96587	8000	As-Sb-Cu-Pb-Ag	NW-trending mesothermal vein swarm
5	Pallatanga	Río Chiguay	6653	96555	-	Hg	Possible tectonic/hydro. breccias
6	Pallatanga	San Gerardo	6514	96666	to 8675	As-Sb-Cd	Mesothermal veins
7	Saraguro	Zaruma-Portovelo	6945	95980	to 9446	Ag-Cu-Pb-Zn-As-Cd-Bi	Structural control rhyolitic complexes
8	Saraguro	Q. Honda	6555	95949	-	Hg	LS epithermal system
9	Saraguro	Tres Chorreras	6637	96498	to 9561	Cu-Mo-As-Sb-Bi	Tourmaline breccias
10	Saraguro	Gigantones	6602	96447	to 3837	Cu-Mo	Tourmaline breccias
11	Saraguro	La Playa	6515	96402	to 2140	W-Cu-Mo-Bi-As-Sb	Tourmaline breccias
12	Saraguro	Mollepungu	6514	96371	3415	Ag-W-Cu-Mo-As-Sb	Tourmaline breccias
13	Saraguro	Cañaribamba	6882	96449	3046	Ag	Rhyolite associated LS epithermal system
14	Saraguro/St. Isabel	Gañarín	6806	96352	1045	None	LS epithermal system
15	Granodiorite	Paccha	6488	96051	5749	Ag-Pb-Cu-Zn-Cd-Bi-Sn-As-Sb	Tourmaline breccias
16	Saraguro	Shagli	7677	96551	-	As	Andesite porphyry
17	Quimsacocha	Quimsacocha	9988	96639	-	As-Cu-Hg	Post-caldera rhyolite
18	Turi	R. Quinuahuaycu	7019	96594	-	Hg	Caldera margin hot spring sinter
19	Turi	R. Cristal	7068	96587	-	Hg	Caldera margin hot spring sinter
20	Saraguro	Q. Cordococha	6799	96579	-	Hg	Post-caldera rhyolite associated epithermal
21	Saraguro	Q. del Salado	-	-	-	Hg	Sinter
22	Saraguro	Q. de Hornillos	6669	96098	-	Hg	LS epithermal system
23	Tarqui	R. Paguishapa	6908	96010	-	As	Unknown source
24	Granodiorite	R. Byron	6261	96120	to 3747	As, Sb, Cu, Pb	Tourmaline breccias
25	Saraguro	Fierro Urcu	6838	95894	-	Cu	Porphyry and stockwork

** additional mineral occurrences in same drainage system

An appropriate reconnaissance model for low-sulphidation epithermal Au within the 3°-4°S area may be derived from conditions prevailing at known prospects such as Cerro Plancharumi (Williams et al., 1997), Cañaribamba, Gañarín, and possibly higher sulphidation systems such as Quimsacocha, where Hg enrichment is commonly marginal to the principal economic target (typically centred on a post-caldera or structurally-controlled rhyolite emplacement). Alteration halos differ significantly. At Quimsacocha, alunite-bearing alteration (a product of a relatively low pH regime) and Fe-Cu-Hg-Au mineralisation occur within a broader area of intense propylitisation. At Gañarín locally intense silicification is evident. At Cañaribamba subtle adularia alteration occurs in virtually unsilicified rocks. These observations may be relevant to the interpretation of the numerous Hg anomalies recorded in the absence of Au or base-metal enrichment, for example in Q. de Hornillos. Mercury enrichment in this highly prospective Gañarín Belt setting may constitute the most easterly geochemical expression of a system structurally constrained within the Río San José Fault zone. A rhyolite intrusion associated with this N-S trending fracture has been mapped 2 km to the west of the anomaly, supporting a metallogenic scenario analogous to that for Cañaribamba.

No equivocal evidence of new mesothermal and/or porphyry-related occurrences is provided by the drainage reconnaissance data for the 3°-4°S area. Emphasis must, therefore, be placed on the improved characterization of documented prospects. Site-specific case-studies conducted under PRODEMINCA sub-component 3.5 (Evaluation of ore-districts) provide a valuable supplement to commercial evaluations such as those ongoing at Gaby (Ecuadorian Minerals Corp) and La Playa (Ecuanor).

6.2 Environmental baselines

6.2.1 Rationale

Drainage geochemistry data, although generated almost exclusively for metalliferous mineral exploration prior to the 1980s, are now recognised as a valuable resource for environmental auditing, risk assessment and land-use planning at scales ranging from site-specific to global. The requirement for internally consistent, national and international multi-element datasets for environmental purposes has provided the impetus for the development of a global geochemical database under IGCP-259 (Darnley et al., 1995). Some possible environmental applications of the dataset compiled for the 3°-4°S sector of the Cordillera Occidental are outlined below.

6.2.2 Development of sediment quality criteria

The state of development of sediment quality criteria is limited relative to the established water quality standards (mostly derived from US-EPA and WHO potable water limits) routinely deployed by environmental regulatory authorities worldwide. In recent studies of mining and urbanization impacts on sediment quality in Ecuador, the Philippines, Indonesia and East Africa (e.g. Williams et al., 1996a, 1996b. 1997b; Appleton et al., 1996) guidelines from the EC Draft Criteria Document (Van Veen and Strotelder, 1988) presented to the International Sediment Quality Forum (1992), and/or the Canadian Sediment Quality Criteria for the Protection of Aquatic Life (Environment Canada, 1992; reviewed in MacDonald, 1994) have been applied. The former are, however, based solely on statistical analysis of sediment data from the Netherlands and thus have no specific human or ecotoxicological significance. The latter (Table 18), although based on modelled and experimental dose-response data, assumes 100% bioavailability for sediment-bound contaminants (although the effect of pH is accommodated, thus accounting for the relatively high Pb toxic effect threshold at pH 7.0) with the result that action thresholds are unrealistically low (see Williams et al., 1997a).

Table 18. Sediment Quality Criteria (mg/kg) for the Protection of Aquatic Life. Source: Environment Canada (1992), reviewed by MacDonald (1994)

Element	No effect threshold	Minimal effect threshold	Toxic effect threshold
As	3	7	17
Cd	0.2	0.9	3
Cu	28	28	86
Pb	23	53	170
Hg	0.05	0.2	1
Zn	100	150	540

The application of universal trace element standards for soil or sediment quality assessment at the regional, national or international scale is now recognised as a weakness in this field of environmental regulation in Europe and North America. Such standards fail to account for the natural (lithologically controlled) variability of ambient environmental concentrations of both micro-nutrients and potentially toxic trace elements. The resultant problems can be exemplified by applying the Sediment Quality Criteria for the Protection of Aquatic Life (Environment Canada, 1992) toxic effect thresholds for As (Table 18) to the 3°-4°S quadrangle, in which median As values range from <5 mg/kg for the Tarqui, Turi and Quimsacocha Formations to >18 mg/kg for the Pallatanga Unit and major intrusive complexes. A threshold of 17 mg/kg thus corresponds to >3 times the background within the former units, yet falls below the background (as defined by the median) for the latter.

A more pragmatic approach to the development of quality criteria for environmental monitoring and protection, now gaining international acceptance, involves the derivation of lithologically normalised background, threshold and action levels for sediment (or soil) contaminants (e.g. Darnley et al., 1995). These provide a basis for assessing the environmental impact of agricultural, industrial and residential developments within their specific local or regional context. The establishment of such normalised thresholds is, however, dependent on the existence of regional or national-scale geological and multi-element geochemical data which depict the natural lithological spectrum. In this respect, the geological mapping and regional reconnaissance programmes conducted in the Cordillera Occidental may directly underpin the development under PRODEMINCA sub-component 2.3 (Policy Development) of national environmental legislation.

6.2.3 Prediction and control of mining impacts

Studies of the hydrochemistry of drainage waters from over fifty Au and complex sulphide operations in Africa and SE Asia (Williams and Breward, 1995) have shown the composition of leachates to be a predictable function of deposit type, ore mineralogy and geological setting (Fig. 9). In addition to defining exploration targets, drainage sediment geochemistry data also elucidate the sulphide composition of the assemblage. Such data therefore provide an early insight into potential geochemical hazards associated with deposit exploitation, of value at the project planning and impact assessment stages.

Within the 3°-4°S sector of the Cordillera Occidental the contrasting geochemical signatures, and hence inherent environmental hazards, associated with prospects of differing metallogenic character are exemplified in Figure 10. The spidergrams (constructed only using elements of economic and/or environmental importance) discriminate, for example, the low-temperature, low-sulphidation Cañaribamba and Gañarín prospects by their Au/base metal ratios. Values of Cu, Pb, Zn, Cd, As and Sb in these locations are characteristically two or three orders of magnitude lower than those associated with tourmaline breccia and mesothermal lode occurrences. Within the mesothermal occurrences for which data are presented, La Playa is uniquely characterised by W enrichment. Although not incorporated in Figure 9, the presence of tellurides (to ca. 80 mg/kg Te) distinguishes Bella Rica from mesothermal assemblages at San Gerardo and elsewhere.

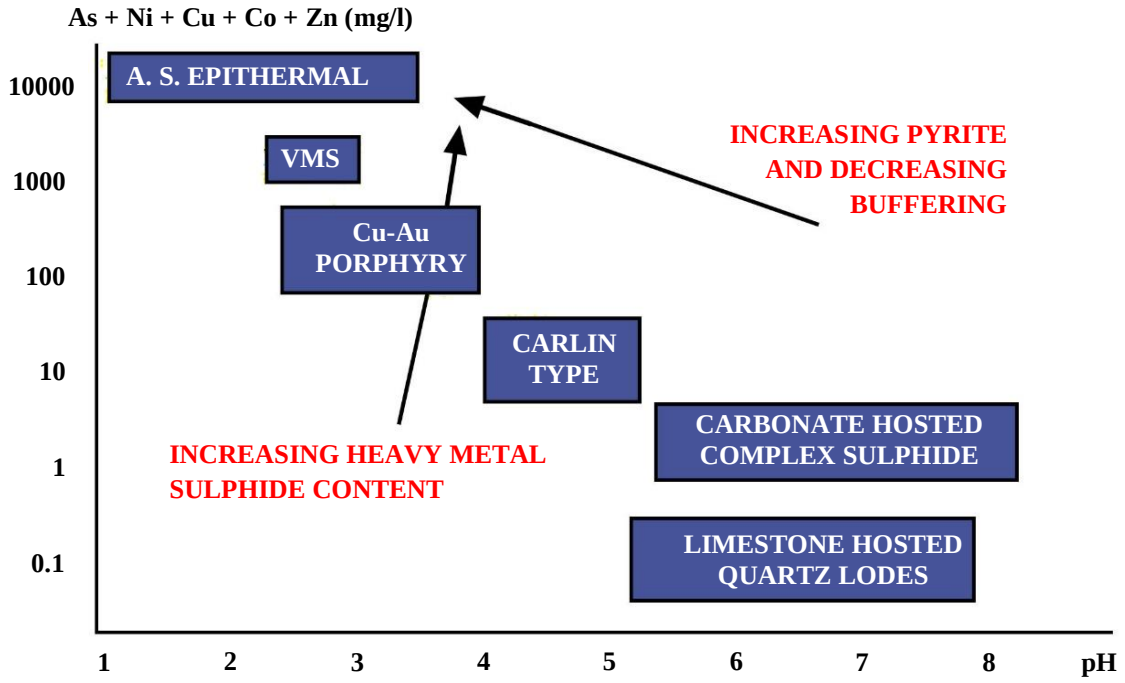

Figure 9. Characteristic pH and dissolved contaminant characteristics of mine-waters associated with contrasting metallogenic settings, based on empirical data from Thailand, Malaysia, Zimbabwe, the Philippines and the USA

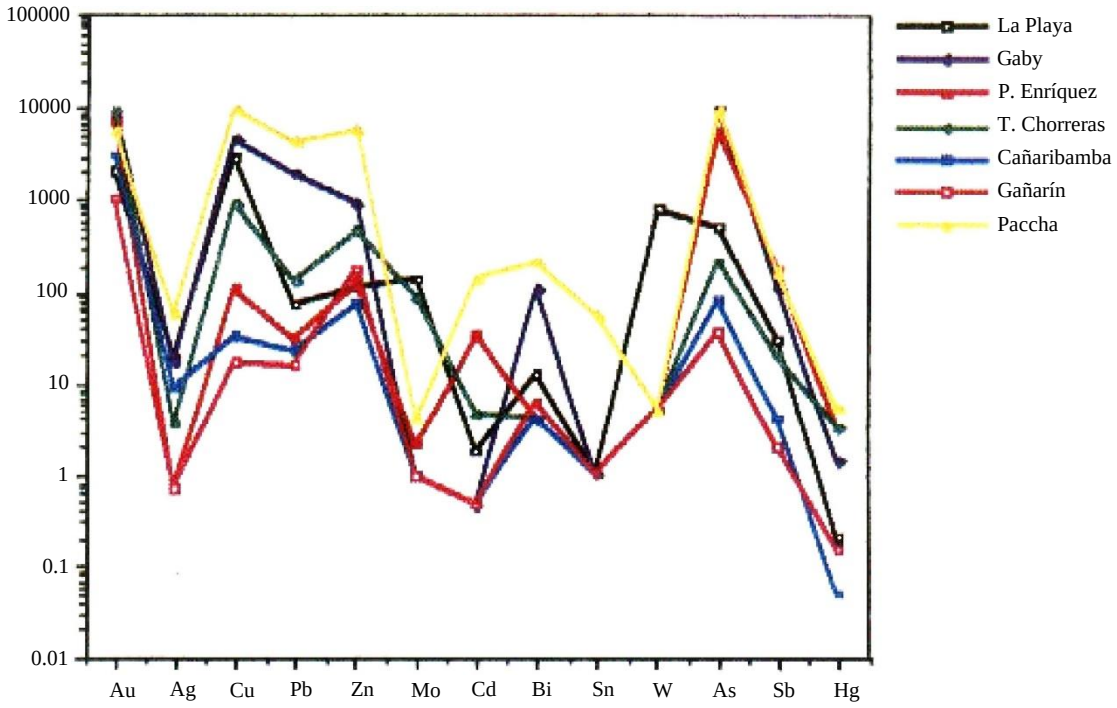

Figure 10. Spidergrams for selected mineral deposits within the 3°-4°S sector of the Cordillera Occidental, constructed using elements of economic and environmental significance

6.2.4 Natural geochemical hazards

The importance of environmental geochemistry in the aetiology of numerous trace element-related diseases has been emphasised by Mills (1996). Lithologically-controlled variations in the concentration of P, I, Se, Cu, Co and other trace elements exert a first-order control on the distribution of numerous animal and/or human diseases related to micro-nutrient deficiency, of which goitre and cretinism related to I-deficiency (e.g. Fuge, 1996) and Se-responsive cardiomyopathic diseases (e.g Mills, 1996) are best documented. Darnley et al. (1995) have shown extensive regions of the world to have natural levels of essential trace elements well below those recommended for agricultural soils and pasture. Chronic toxicity problems (in humans and/or livestock) associated with natural exposure to F (notably East Africa), As (India, Bangladesh, Thailand, Argentina, Mexico, Chile, Uruguay) and Se (China, USA) are also widely known (e.g. Plant et al., 1996).

Within the context of human and animal health, potentially significant natural geochemical features of the 3°-4°S quadrangle include areas of intense Mo enrichment (to 200×mean upper crustal abundance) in the La Playa and Tres Chorreras localities, and localised Hg enrichment (to 600×mean upper crustal abundance) in association with numerous low-temperature palaeospring or sinter exhalations, notably south of Quimsacocha. High environmental Mo levels (typically restricted to Cu-Mo porphyry systems and black shales) are a potential cause of secondary Cu deficiency through the inhibition of Cu assimilation in ruminants (Mills, 1996). The influence is strongly pH-dependent, and further characterization of local physico-chemical conditions is necessary to fully evaluate the risk. With respect to Hg, peak values recorded as natural features in systems such as the Río Quinuahuaycu exceed those reported for the Nambija (Williams and Orbea, 1997), Ponce Enríquez (Appleton et al., 1996) and Zaruma-Portovelo mining fields by up to a factor of 10. These natural anomalies lie within the upper range of sediment values documented for major gold-rush localities in Brazilian Rondonia and Venezuela (Pfeiffer et al., 1989; 1991; Martinelli et al., 1988).

6.3 Concluding statement

All data incorporated within this document were compiled in accordance with the specific objectives of PRODEMINCA sub-component 3.4 (Thematic Mapping), and the broader PRODEMINCA goals outlined in the Project Memorandum of the World Bank (1993). To achieve the latter, the integration of geochemical data with geoscientific, social and economic outputs of other project sub-components is a central requirement. Probable areas of application for geochemical reconnaissance data (excluding exploration) within the context of PRODEMINCA include Policy Development (2.3), Monitoring of Pollution and Health Related to Mining Activities (3.1), Containment and Neutralization of Hazardous Mining Wastes (3.2), Geological Mapping (3.3), Assessment of Ore Districts (3.5) has been indicated in sections 6.1-6.3 of this report. Utilisation of geochemical information within these sub-components has been facilitated to the greatest possible extent under the current programme by the adoption of an Oracle database and Intergraph GIS, compatible with IT systems used under all other technical PRODEMINCA sub-components.

The function of this document as a methodological/data overview is outlined in section 1. Following the 1998 release of digital geochemical data for the 3°-4°S and 2°-3°S areas of the Cordillera Occidental, the strategic and economic return will be determined largely by private sector interest. The demand for the involvement of CODIGEM, DINAPA, DINAMI and other government departments in data management, the provision of multi-thematic datasets and interpretive guidance will, however, remain. This longer-term public-sector contribution may ultimately be no less important than private investment in achieving the central PRODEMINCA goal of sustainable development of Ecuador's metalliferous minerals sector.

7. BIBLIOGRAPHY

APPLETON J. D. (1996) Assessment of mercury contamination in the Ponce Enríquez artisanal gold mining area, Ecuador. British Geological Survey, Overseas Geology Series Technical Report WC/96/55.

ASPDEN J. A., HARRISON S. M. and RUNDLE C. C. (1992) New geochronological control for the tectono-magmatic evolution of the metamorphic basement. Cordillera Real and El Oro province of Ecuador. Journal of South American Earth Sciences, Vol. 6, 77-96.

ASPDEN J. A., BONILLA W. and DUQUE P. (1995) The El Oro metamorphic complex, Ecuador: Geology and economic mineral deposits. Overseas Geology and Mineral Resources, No. 67, 63pp.

BALDOCK J. W. (1982) Geología del Ecuador. Boletín de la explicación del mapa geológico (1:1000000) de la República del Ecuador. Ministerio de Recursos Naturales y Energéticos, Quito, 54pp.

BOLVIKEN B. and SINDING-LARSEN B. (1973) Total error and other criteria in the interpretation of stream sediment data. In: Geochemical Exploration 1972 (London: Institution of Mining and Metallurgy).

BRITISH GEOLOGICAL SURVEY and CORPORACIÓN DE DESARROLLO e INVESTIGACIÓN GEOLÓGICO, MINERO y METALÚRGICO (1997) Geological map of the Western Cordillera, Ecuador between 3 and 4 degrees south (1:200000). BGS, Keyworth, UK.

DARNLEY A. G., BJORKLUND A., BOLVIKEN B., GUSTAVSSON N. and KOVAL P. (1995) A global geochemical database: Recommendations for international geochemical mapping. Final report of IGCP project 259. UNESCO, Paris.

DIRECCIÓN NACIONAL DE GEOLOGÍA Y MINAS (1973a) Mapa Geológico del Ecuador.

DUNKLEY P. N., GAIBOR A. and BOLAÑOS J. E. (1997) Geochemical orientation survey, Río Junín. Geological Information Mapping Programme (GIMP) report No. 5. World Bank Mining Development and Environmental Control Project (PRODEMINCA), Misión Geológica Británica, CODIGEM, Quito, Ecuador.

DUNKLEY P. N. and GAIBOR A. (1997a) Control of quality of geochemical data. Geological Information Mapping Programme (GIMP) report No. 6. World Bank Mining Development and Environmental Control Project (PRODEMINCA), Misión Geológica Británica, CODIGEM, Quito, Ecuador.

DUNKLEY P. N. and GAIBOR A. (199b) Geology of the area between 2 and 3 degrees south. Western Cordillera, Ecuador. Open File Report WC/97/26, British Geological Survey.

FEININGER T. (1973) Geologic map of the western part of the El Oro Province (1:50000). Escuela Politécnica Nacional, Quito, Ecuador.

FUGE R. (1996) Geochemistry of iodine in relation to iodine deficiency diseases. In: Environmental geochemistry and health with special reference to developing countries. Geological Society Special Publication No. 113, 201-213. Geological Society of London.

GARRETT R. G. (1983) Sampling methodology. In: Howarth R. J. Ed. Handbook of exploration geochemistry volume 2: Statistics and data analysis in geochemical prospecting. Chapter 4, 83-111. Elsevier, London.

GEMUTS I., LÓPEZ G. and JIMÉNEZ F. (1982) Gold deposits of southern Ecuador. Newsletter of the Society of Economic Geologists, No. 11, 13-17.

GOOSSENS P. J. (1972) An exhalative volcanic iron sulphide stratabound deposit near San Fernando, Azuay Province, Ecuador. Economic Geology, Vol. 67, 469-480.

HUGHES R. A. and BERMÚDEZ R. A. (1997) Geology of the area between 1 degree south and the equator, Western Cordillera, Ecuador. Open file report WC/97/25, British Geological Survey.

HUNGERBÜHLER D. and STEINMANN M. (1996) Curso internacional geología de cuencas sedimentarias (Mioceno, Sur del Ecuador). Guía del campo. Escuela Politécnica Federal de Zürich, 27.

HUNGERBÜHLER D. and STEINMANN M. (in prep) Tertiary basins in the Andes of southern Ecuador (3°S-4°20’S): Sedimentary evolution, deformation and regional tectonic implications. Unpublished PhD Thesis. Institute of Geology, Zürich, Switzerland.

JAILLARD E., ORDÓÑEZ M., BERRONES G., BENGTSON P., BONHOMME M., JIMÉNEZ N. and ZAMBRANO I. (1996) Sedimentary and tectonic evolution of the arc zone of southwestern Ecuador during late Cretaceous and early Tertiary times. Journal of South American Earth Sciences, Vol.9, 131-140.

KENNERLEY J. B. (1980) Outline of the geology of Ecuador. Institute of Geological Sciences. Overseas Geology and Mineral Resources, No. 55, 20 pp.

MACDONALD D. D. (1994) A review of environmental quality criteria and guidelines for priority substances in the Fraser River basin. DOE-FRAP. 1994-30.

MARTINELLI L. A., FERREIRA J. R., FORSBERG B. R. and VICTORIA R. L. (1988) Mercury contamination in the Amazon: a gold rush consequence. Ambio, 17 No. 4, 252-254.

MCCOURT W., DUQUE P. and PILATASIG L. (1997) Geology of the Cordillera Occidental of Ecuador between 1° and 2° S. Geological Information Mapping Programme (GIMP) Report No. 3. World Bank Mining Development and Environmental Control Project (PRODEMINCA). Misión Geológica Británica, CODIGEM, Quito, Ecuador.

MILLS C. F. (1996) Geochemical aspects of the aetiology of trace element related diseases. In: Environmetal geochemistry and health with special reference to developing countries. Geological Society Special Publication No. 13, 113, 1-7. Geological Society of London.

MISIÓN BELGA (1989) Informe de evaluación técnica complementaria del área minera Portovelo. Proyecto del sector minero en el Ecuador. INEMIN/AGDC.

NAKASHIMA S. (1979) Selective determination of arsenic (iii) and arsenic (v) by atomic absorption spectrophotometry following arsene generation. Analyst. Vol. 104, pp. 172-173.

PALADINES A. and ROSERO G. (1996) Zonificación mineralógica del Ecuador. (Laser editores; Quito).

PFEIFFER W. C., LACERDA D. L., MALM O., SOUZA C. M. M., DE SILVA E. G. and BASTOS W. R. (1989) Mercury concentrations in inland waters of gold mining areas in Rondonia, Brazil. Science of the Total Environment. 78, 233-240.

PFEIFFER W. C., MALM O., SOUZA C. M. M., LACERDA D. L., DE SILVA E. G. and BASTOS W. R. (1991) Mercury in the Madeira River ecosystem. Rondonia, Brazil. Forest Ecology and Management, 38, 239-245.

PLANT W. C. (1973) A random numbering system for geochemical samples. Transactions of the Institution of Mining and Metallurgy, section B. 83.

PLANT J. A. and MOORE P. J. (1979) Regional geochemical mapping and interpretation in Britain. Philosophical Transactions of the Royal Society of London, Vol. 288, B95-112.

PLANT J. A., JEFFREY J. K., GRILL E. and FAGE C. (1975) The systematic determination of error, accuracy and precision in geochemical exploration data. Journal of Geochemical Exploration, Vol. 4, 467-486.

PLANT J. A., BALDOCK J. W. and SMITH B. (1996) The role of geochemistry in environmental and epidemiological studies in developing countries: a review, In: Environmental geochemistry and health with special reference to developing countries. Geological Society Special Publication No. 113, 7-23. Geological Society of London.

PRATT W. T., FIGUEROA J. F. and FLORES B. G. (1997) Geology of the Cordillera Occidental of Ecuador between 3° and 4° S. Geological Information Mapping Programme (GIMP) Report No. 1. World Bank Mining Development and Environmental Control Project (PRODEMINCA), Misión Geológica Británica, CODIGEM, Quito, Ecuador.

THOMPSON M. and HOWARTH R. J. (1978) A new approach to the estimation of analytical precision. Journal of Geochemical Exploration, 9, 23-30.

UNITED NATIONS DEVELOPMENT PROGRAMME (1969) Survey of metallic and non-metallic minerals. Iron-sulphide mineralization, San Fernando, Azuay Province. *Technical Report, United Nations Development Programme, Quito-New York.*

VAN THOURNOUT F., VALENZUELA G., MERLYN M. and SALEMINK J. (1991) Portovelo, mineralización epitermal en relación con una caldera. Boletín Geológico Ecuatoriano, Vol. 2, 13-26.

VAN VEEN R. J. and STROTELDER P. B. M. (1988) Research on contaminated sediments in the Netherlands. In Wolf K., Van de Brink W. J. and Colon F. J. (Eds). Contaminated soil. 1263-1275. Academic Publ.

WILLIAMS T. M., ROBOTHAM H. and SIMPSON P. R. (1992) Soil geochemistry of the Central, Above Rocks and Blue Mountains inliers and intervening Cenozoic sequences. Jamaica. British Geological Survey Geochemistry Series Technical Report WP/92/13/R.

WILLIAMS T. M. and BREWARD N. (1995) Environmental impacts of gold and complex sulphide mining (with particular reference to arsenic contamination). British Geological Survey Overseas Geology Series Technical Report WC/95/2.

WILLIAMS T. M., WEEKS J. M., APOSTOL A. and MIRANDA C. (1996a) Assessment of mercury toxicity hazard associated with cinnabar mining and tailings disposal in Honda Bay,

Palawan, Philippines. British Geological Survey. Overseas Geology Series Technical Report WC/96/31/R.

WILLIAMS T. M., REES J. G., KAIRU K. K. and YOBE A. C. (1996b) Assessment of contamination by metals and selected organic compounds in coastal sediments and waters of Mombasa, Kenya. British Geological Survey. Overseas Geology Series Technical Report WC/96/37.

WILLIAMS T. M. and ORBEA H. (1997) Dispersal of mercury and ore-derived metals in surface drainage of the Nambija artisanal mining field, Ecuador. British Geological Survey. Overseas Geology Series Technical Report WC/97/37.

WILLIAMS T. M., FORDYCE F. M., PAIJITPRAPAPON A. and CHAROENCHAISRI P. (1995b) Arsenic contamination in surface drainage and groundwater in part of the Southeast Asia tin belt. Nakhon si Thammarat Province, Southern Thailand, Environmental Geology, 27, 16-33.

WILLIAMS T. M., DUNKLEY P. N. and GAIBOR A. (1997a) Drainage reconnaissance of the Cordillera Occidental of Ecuador between 2°-3°S. Geological Information Mappings Programme (GIMP) Report No. 7. World Bank Mining Development and Environmental Control Project (PRODEMINCA), Misión Geológica Británica, CODIGEM, Quito, Ecuador.

WILLIAMS T. M., REES J. and SETIAPERMANA D. (1997b) Land-derived contaminant influx to Jakarta Bay, Indonesia, Volume 1: Geochemistry of marine water and sediment. British Geological Survey. Overseas Geology Series Technical Report WC/97/19.

WOODS M. A. (1997) Biostratigraphical interpretation of macrofaunas from Ecuador. Technical Report WH/97/13R, Biostratigraphy and Sedimentology Group, British Geological Survey.